СИБИРСКОЕ ОТДЕЛЕНИЕ
РОССИЙСКОЙ АКАДЕМИИ НАУК

НАУЧНЫЙ ЖУРНАЛ
ГЕОЛОГИЯ И ГЕОФИЗИКА

Геология и геофизика, 2018, т. 59, № 1, с. 3—22

ПЕТРОЛОГИЯ, ГЕОХИМИЯ И МИНЕРАЛОГИЯ

УДК 551.22(519.3)

СРАВНЕНИЕ МАФИТОВЫХ-УЛЬТРАМАФИТОВЫХ ИНТРУЗИВОВ ООРТСОГ, ДУЛААН И НОМГОН В ЦЕНТРАЛЬНОЙ МОНГОЛИИ И МЕСТОРОЖДЕНИЙ Ni-Cu РУД В СЕВЕРО-ЗАПАДНОМ КИТАЕ: ВЫВОДЫ ДЛЯ ПРОМЫШЛЕННОЙ РАЗВЕДКИ Ni-Cu-ЭПГ РУДНЫХ ЗАЛЕЖЕЙ В ЦЕНТРАЛЬНОЙ МОНГОЛИИ

Я-Цзин Мао[1], Даш Бат-Ульзии[2], Кэ-Чжан Цинь[1,3], Бойджирын Буджинлхем[2], Дун-Мэй Тан[1]

[1] Key Laboratory of Mineral Resources, Institute of Geology and Geophysics, Chinese Academy of Sciences, Beijing 100029, China
[2] Department of Geology and Mineralogy, Mongolian University of Science and Technology, Ulaanbaatar-46/520, Mongolia
[3] University of Chinese Academy of Sciences, Beijing 100049, China

В Западной и Центральной Монголии, расположенной в Центрально-Азиатском складчатом поясе (ЦАСП), развиты многочисленные мафит-ультрамафитовые интрузии, но промышленные месторождения Ni-Cu-руд пока не выявлены. Для оценки промышленного никель-медного рудного потенциала интрузивов в Центральной Монголии исследуются родственная связь родоначальных магм и насыщенность сульфидами мафит-ультрамафитовых интрузивов Оортсог, Дулаан и Номгон с Ni-Cu минерализацией. В трех интрузивах преобладают габбровые породы, а интрузивы Оортсог и Дулаан содержат небольшие количества перидотитов. Интрузивы Оортсог и Дулаан сформировались из толеитовых магм, о чем свидетельствует состав их Cr-шпинели и клинопироксена, в то время как родоначальная магма интрузива Номгон была, вероятно, щелочного состава. Кроме того, низкое содержание Ca в оливине (<500 г/т), а также его значительная обедненность Nb и Ta свидетельствуют, что породы образовались, скорее всего, из преобразованных мантийных источников. По составу оливина интрузивы Оортсог и Номгон подразделяются на два кластера, что указывает на многократное внедрение магм. Относительно низкие значения Fo и содержания Ni в оливине трех интрузивов по сравнению с таковыми в никель-медных месторождениях Северо-Западного Китая, а также в месторождении Войси-Бей в Канаде указывают на то, что все три интрузии были кристаллизованы из относительно развитых магм. Отношения Cu/Zr в породах интрузивов Оортсог, Дулаан и Номгон выше 1, таким образом, породы, вероятно, содержат сульфидный кумулус. Исходя из этого факта, а также присутствия округлых сульфидных включений в оливине интрузивов Оортсог и Дулаан, можно предположить, что насыщение пород сульфидами происходило до или во время кристаллизации оливина. Отношение Ni/Cu в сульфидсодержащих породах интрузива Оортсог варьирует от 1.8 до 3.8, что согласуется с аналогичными отношениями в месторождениях Ni-Cu сульфидных руд Северо-Западного Китая. Напротив, отношения Ni/Cu в сульфидсодержащих породах интрузива Номгон очень низкие (0.03–0.07), что указывает на то, что сульфиды выделились из магмы, высокообогащенной Cu, но обедненной Ni. В целом, хотя родоначальные магмы интрузивов в Центральной Монголии более развиты, чем магмы интрузивов в Северо-Западном Китае, эти интрузивы сопоставимы по размерам, минеральному составу и химическому составу минералов. Эти сходства свидетельствуют о том, что интрузивы Центральной Монголии перспективны на промышленные месторождения Ni-Cu сульфидных руд.

Месторождение Ni *и* Cu*, элементы платиновой группы, разведка, основная—ультраосновная интрузия, Центрально-Азиатский складчатый пояс, Центральная Монголия.*

COMPARISON AMONG THE OORTSOG, DULAAN, AND NOMGON MAFIC–ULTRAMAFIC INTRUSIONS IN CENTRAL MONGOLIA AND Ni–Cu DEPOSITS IN NW CHINA: IMPLICATIONS FOR ECONOMIC Ni–Cu–PGE ORE EXPLORATION IN CENTRAL MONGOLIA

Y.-J. Mao, D. Bat-Ulzii, K.-Z. Qin, B. Bujinlkham, and D.-M. Tang

Although there are many mafic–ultramafic intrusions in the western and central regions of Mongolia, Central Asian Orogenic Belt (CAOB), no economic-grade Ni–Cu deposits have yet been discovered. To understand the economic Ni–Cu deposit potential of the intrusions in central Mongolia, the parental magma affinity and sulfide saturation of the Oortsog, Dulaan, and Nomgon Ni–Cu mineralized mafic–ultramafic intrusions are studied. These three intrusions are predominantly gabbroic in composition, while the Oortsog and Dulaan in-

✉e-mail: maoyajing@mail.iggcas.ac.cn
DOI: 10.15372/GiG20180101

trusions additionally contain small proportions of peridotites. The parental magmas of the Oortsog and Dulaan intrusions are tholeiitic, as indicated by their Cr-spinel and clinopyroxene compositions, whereas the parental magma of the Nomgon intrusions is likely calc-alkaline. The compositions of Cr-spinel and clinopyroxene, combined with significant Nb–Ta depletion, indicate that these rocks were most likely derived from modified mantle sources. Both the Oortsog and Nomgon intrusions form two clusters in terms of their olivine composition, suggesting that multiple magma surges were involved during their emplacement. The relatively low Fo values and Ni contents in olivine from the three intrusions compared to those from Ni–Cu deposits in NW China, as well as those in the Voisey's Bay deposit in Canada, indicate that the three intrusions crystallized from relatively evolved magmas. The Cu/Zr ratios of rocks of the Oortsog, Dulaan, and Nomgon intrusions are higher than 1, suggesting that these rocks contain cumulus sulfide. This, coupled with the presence of rounded sulfide inclusions in olivine of the Oortsog and Dulaan intrusions, suggests that sulfide saturation occurred before or during olivine crystallization. The distribution patterns of platinum group elements (PGEs) of the Dulaan and Oortsog intrusions record slight Rh, Pt, and Pd (PPGE) enrichment relative to Os, Ir, and Rh (IPGE). Furthermore, the Ni/Cu ratios of sulfide-bearing rocks from the Oortsog intrusion vary from 1.8 to 3.8 and are consistent with those of the Ni–Cu sulfide deposits in NW China. In contrast, the Ni/Cu ratios of sulfide-bearing rocks from the Nomgon intrusion are extremely low (0.03 to 0.07). This, together with the significant enrichment in PPGE relative to IPGE, suggests that these sulfides of the Nomgon intrusion were segregated from a magma that was extremely enriched in Cu and PPGE but depleted in Ni and IPGE. The characteristics of the chalcophile elements in these intrusions are attributed to the fact that the derivation of the Nomgon magma was significantly different from that of the Dulaan and Oortsog parental magmas. Overall, although the parental magmas of the intrusions in central Mongolia are more evolved than those in NW China, they are comparable in the sizes of their intrusions, constituent minerals, and mineral chemistry. These similarities suggest that the intrusions in central Mongolia have an economic Ni–Cu sulfide potential. Furthermore, intrusions similar to the Nomgon intrusion may feature a PGE mineralization potential.

Ni–Cu *deposit, platinum group elements, exploration, mafic–ultramafic intrusion, Central Asian Orogenic Belt, central Mongolia*

INTRODUCTION

In recent decades, the occurrence of magmatic Ni-Cu sulfide deposits in orogenic belts has been widely reported (Li et al., 2015; Maier et al., 2008; Maier et al., 2016), suggesting that orogenic belts are capable of future Ni-Cu sulfide deposit exploration. The Central Asian Orogenic Belt (CAOB), also known as the Altaid Tectonic Collage, which is bounded by the Siberian craton to the north and the Tarim-North China cratons to the south (Fig.1a), represents a complex evolution of Phanerozoic orogenic belts (Sengör et al., 1993; Windley et al., 2007; Xiao et al., 2004). Numerous Ni-Cu sulfide deposits have been discovered in the southern margin of the CAOB in China since the 1980s. Although many mafic-ultramafic intrusions featuring Ni-Cu and/or platinum group element (PGE) mineralization in the central part of CAOB in Mongolia have been documented on the metallogenic map of Mongolia (Dejidmaa et al., 2001) and in the literature (Izokh et al., 1998; Izokh et al., 1990; Kozakov et al., 2007; Oyunchimeg et al., 2009; Polyakov et al., 2008), the potential of the Ni-Cu-PGE deposit within these intrusions remains ambiguous.

Studies of world-class magmatic Ni-Cu deposits reveal that the following factors are essential for generating economic Ni-Cu deposits (Barnes et al., 2016; Naldrett, 2010a; Naldrett, 2010b): 1) parental magmas, derived from a mantle source, with moderate to high Ni concentrations, 2) sulfide saturation induced by the addition of crustal sulfur and/or crustal contamination, and 3) sulfide accumulation in a dynamic environment. Olivine and Cr-spinel are two minerals that crystallize early in basaltic and komatiitic magmas, therefore, their compositions can be used to indicate the composition of their parental magma (Barnes et al., 2013; Barnes and Roeder, 2001; Sobolev et al., 2007). In addition, the variation of Ni content in olivine is strongly associated with magma evolution and sulfide segregation, because Ni is compatible in olivine and strongly partitions into sulfide melt during magma evolution (Barnes et al., 2013; Li et al., 2000; Li and Naldrett, 1999; Li et al., 2007; Li et al., 2001), and is thus a useful indicator of the sulfide saturation process.

In this study, we study the petrology, whole rock PGE, and mineral compositions of the Oortsog, Dulaan, and Nomgon intrusions in central Mongolia to characterize the parental magma composition and sulfide saturation conditions of these intrusions. These data are then compared with published data of other economic Ni-Cu deposits in NW China, as well as Ni-Cu deposits worldwide, to better constrain the economic Ni-Cu deposit potential of these intrusions. The aim of this study is to shed light on the exploration of magmatic Ni-Cu-PGE deposits in central Mongolia.

GEOLOGICAL BACKGROUND

Based on its tectonostratigraphic, Mongolia can be subdivided into an Early Paleozoic domain in the north and a Late Paleozoic domain in the south (Fig. 2) (Badarch et al., 2002; Windley et al., 2007). The Early

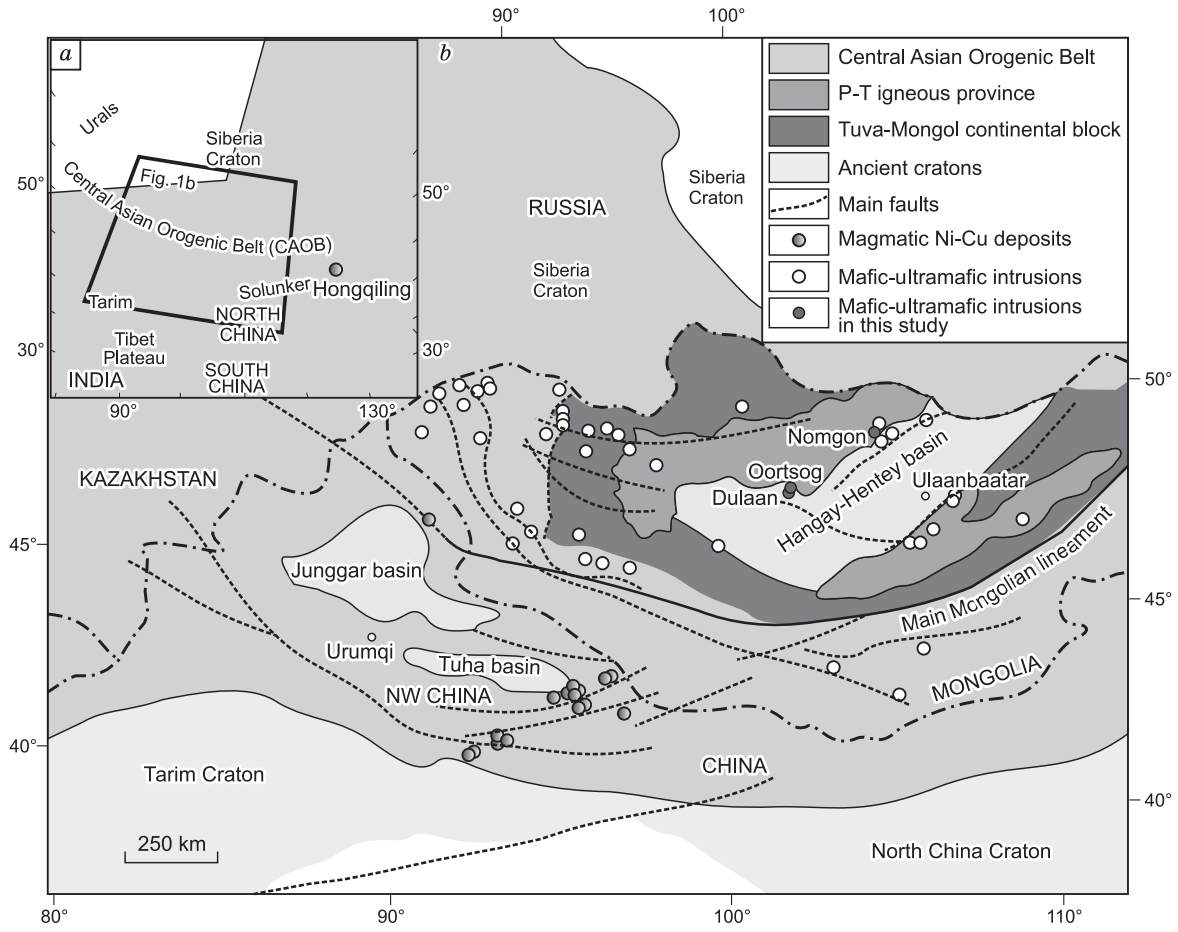

Fig. 1 Simplified map of the Central Asian Orogenic belt, after (Sengör et al., 1993) (*a*). Distribution of mafic-ultramafic intrusions in Mongolia and magmatic Ni-Cu deposits in NW China (*b*).

Data source: Ni-Cu deposits in NW China (Mao et al., 2008; Mao et al., 2015; Mao et al., 2014a; Qin et al., 2011; Qin et al., 2003; Song and Li, 2009; Su et al., 2011; Xia et al., 2013; Zhang et al., 2009; Zhou et al., 2004), magmatic Ni-Cu deposits in NE China are from (Wei et al., 2015; Wei et al., 2013), mafic-ultramafic intrusion in Mongolia (Dejidmaa et al., 2001), outlines of the Hangay-Hentey basin, Tuva-Mongol continental block, Permian-Triassic (P-T) igneous province (Kelty et al., 2008) and main faults (Badarch et al., 2002).

Paleozoic domain in the north mainly consists of the Hangay–Hentey Basin, the Precambrian Tuva-Mongol continental block, and two Permian-Triassic igneous provinces. The Hangay–Hentey Basin is sandwiched by the Tuva–Mongol block, with two large Permian-Triassic igneous provinces located on the northern and southern rims of the basin (Fig. 1). The block forms a tight "V" in map view, opening towards the east, and is considered to have been either a microcontinent in the Paleo-Asian Ocean in the Late Proterozoic and Cambrian (Kelty et al., 2008; Sengor and Natalin, 1996), or a composite tectonic unit that is composed of several smaller continental blocks (Badarch et al., 2002). The northern arm of the Tuva-Mongol continental block consists of gneiss, migmatite, amphibolite, and schist. The basement is overlain by limestone and volcanic rocks, as well as marine strata interbedded with andesite and rhyolite. The southern arm of the Tuva–Mongol continental block consists of tonalitic gneiss, granulite, amphibolite, minor quartzite, and granodioritic dikes. The basement is overlain by a metasedimentary sequence, and both are overlain by limestone, conglomerate, and sandstone, shale, volcanic rocks interlayered with marine strata, and clastic sediments (Badarch et al., 2002; Kelty et al., 2008). The Hangay–Hentey Basin is primarily composed of Devonian to Carboniferous turbidites that were folded and faulted and intruded or overlain by Mesozoic and Cenozoic igneous rocks (Kelty et al., 2008). The basin is floored by either an enriched mantle lithology or a Precambrian basement, as indicated by the Permian granitic intrusion (Jahn et al., 2004). One of the Permian-Triassic igneous provinces consists of differentiated Permian basalt-andesite-dacite-rhyolite, and the other contains Permian-Triassic trachybasalt (Yarmolyuk and Kovalenko, 1991). The mafic-ultramafic intrusions with Ni-Cu (PGE) mineralization in central Mongolia are distributed at the rims of the Hangay–Hentey Basin and the Permian-Triassic igneous province, as well as inside the Tuva–Mongol continental block (Fig. 1*b*).

In the CAOB, economic Ni-Cu deposits are mainly distributed in NW China, including the Heishan, Huangshanxi, Huangshandong, Huangshannan, Xiangshan, Hulu, Tulaergen, Tianyu and Baishiquan, Poyi, Poshi and Kalatongke deposits (Fig. 1b) (Mao et al., 2008; Mao et al., 2015; Mao et al., 2014a; Qin et al., 2011; Qin et al., 2003; Song and Li, 2009; Su et al., 2011; Sun et al., 2013; Tang et al., 2011; Xia et al., 2013; Xie et al., 2012; Zhang et al., 2009; Zhou et al., 2004), whereas some, such as the Hongqiling and Piaohecheng deposits, are distributed in NE China (Fig. 1a) (Wei et al., 2015; Wei et al., 2013). The deposits in NW China formed from the Devonian to the Permian (Qin et al., 2003; Xie et al., 2012), whereas those in NE China formed during the Jurassic (Wei et al., 2015; Wei et al., 2013). All of these deposits are mainly distributed adjacent to the main faults, which are most likely trans-crustal structures in different tectonic units (Fig. 1b). They are related to small scale intrusions that are composed of mafic (i.e., olivine gabbronorite, gabbronorite) and ultramafic rocks (i.e., lherzolite, plagioclase lherzolite, olivine websterite, websterite) (Qin et al., 2012). The parental magmas of the economic Ni-Cu deposits are H_2O-rich as indicated by the ubiquitous occurrence of magmatic hornblende and phlogopite in these intrusions (Mao et al., 2015; Mao et al., 2014a; Tang et al., 2013).

GEOLOGY AND PETROGRAPHY OF THE OORTSOG, DULAAN, AND NOMGON MAFIC-ULTRAMAFIC INTRUSIONS

The Oortsog and Dulaan intrusions, which outcrop 1.5 km apart, are located in the northern margin of the Hangay–Hentey Basin, close to the southern margin of the Permian-Triassic igneous province. In contrast, the Nomgon intrusion is located at the southern margin of the Permian-Triassic igneous province (Fig. 1*b*). Zircon U-Pb dating indicates that the emplacement age of the Dulaan and Oortsog intrusions is ~270 Ma, whereas the age of the Nomgon intrusion is ~252 Ma (Shelepaev et al., 2015). The distance between the Oortsog and Nomgon intrusions is approximately 300 km. The surface areas of the Oortsog and Dulaan intrusions are approximately 2.5 km^2 and 4 km^2, respectively (Fig. 2). They are hosted by metamorphosed rocks that have been dated as Precambrian. The two intrusions are bordered by mainly gneiss and leucogranite. Numerous granite dikes have intruded the Dulaan intrusion, and a subtle intrusive granite dike is present within the southern margin of the Oortsog intrusion (Izokh et al., 1990). Xenoliths of host rock are widely present in the rim of these two intrusions (Fig. 2). Gneiss xenoliths preserve the lineation in the rim of the Oortsog intrusion. The Nomgon intrusion is approximately 3.8 km long and 2.5 km wide (Fig. 3) and its country rocks mainly consist of porphyritic biotite-hornblende granite, fine-grained granite, granodiorite, and quartz monzonite.

The Oortsog intrusion is composed of ultramafic units (lherzolite) and a mafic unit (mela-olivine gabbronorite, olivine gabbronorite, and gabbronorite) (Izokh et al., 1990). We defined the olivine gabbronorite that have >20% olivine as mela-olivine gabbronorite. The lherzolite unit occurs as an irregular, sheet-like body within the mafic unit (Fig. 2) and has been severely altered into serpentine, which shows poikilitic texture (Fig. 4*a*). This lherzolite is composed of 60 vol.% olivine, 5% orthopyroxene, 5% clinopyroxene, 5% hornblende, ~2% plagioclase and trace amounts of Cr-spinel and sulfides (<1%). The olivine crystals in the lherzolite are characterized as pseudomorphs and a few fresh crystals included in clinopyroxene. Clinopyroxene and hornblende commonly occur as grains interstitial to olivine. Mela-olivine gabbronorite is commonly composed of olivine (20-30%), orthopyroxene (10-20%), clinopyroxene (25-35%), hornblende (10%), plagioclase (10-25%) and minor Cr-spinel (<0.5%). Olivine and clinopyroxene in mela-olivine gabbronorite are commonly subhedral, whereas plagioclase commonly occurs as interstitial grains or small inclusions in olivine and pyroxene (Fig. 4*b*). The textures and mineral assemblages of olivine gabbronorite are identical to these of mela-olivine gabbronorite. However, in olivine gabbro, the proportion of olivine de-

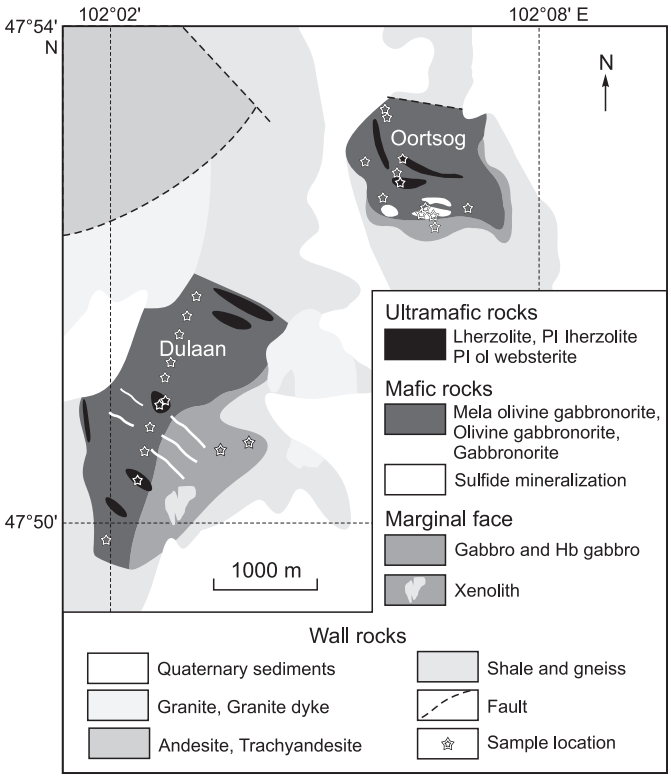

Fig. 2. Simplified geological map of the Oortsog and Dulaan mafic-ultramafic intrusions in central Mongolia (after [Izokh et al., 1990]).

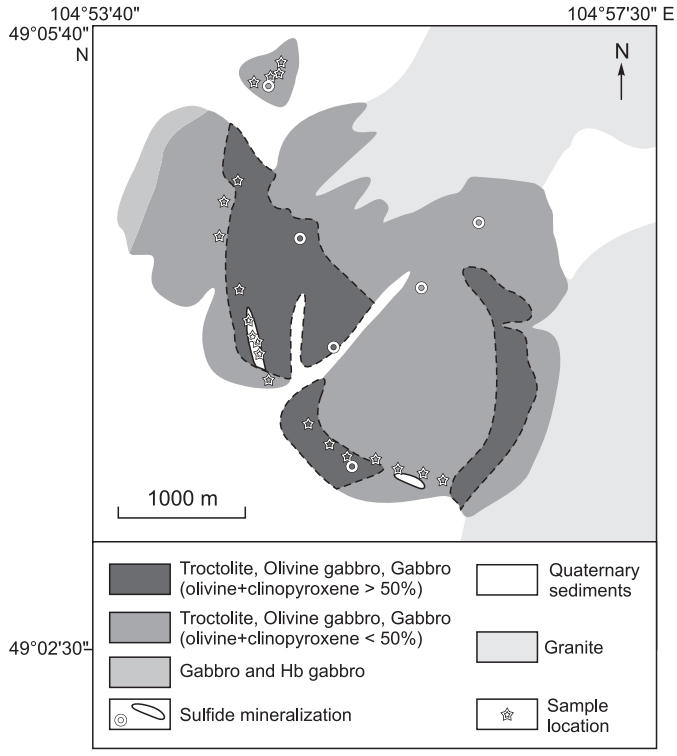

Fig. 3. Simplified geological map of the Nomgon mafic intrusion in central Mongolia (after [Izokh et al., 1990]).

creases to 10-15%, whereas its plagioclase content increases up to 20-60% (Fig. 4*c*). Sulfide mineralization is present in the mafic unit and is exposed in the southern region of the intrusion (Fig. 2). Round sulfide inclusions are present in the olivine of the olivine gabbronorite (Fig. 4*e*). Disseminated sulfides predominantly occur in mela-olivine gabbronorite, in which the sulfide assemblage is mainly composed of pyrrhotite, chalcopyrite, and pentlandite (Fig. 4*f*).

The Dulaan intrusion consists of a bulk mafic unit and some small, irregular ultramafic units (Fig. 2) (Izokh et al., 1990). The ultramafic units comprise plagioclase lherzolite (Pl lherzolite) and plagioclase-olivine websterite (pl-ol websterite). The main mafic unit is composed of olivine gabbronorite, gabbronorite and hornblende gabbro (Hb gabbro). The Pl lherzolite commonly consists of 50-55% olivine, 5% orthopyroxene, 10-25% clinopyroxene, 10-15% hornblende, 10% plagioclase, and minor Cr-spinel plus sulfides (<1%). Olivine in Pl lherzolite occurs as a cumulus phase, whereas clinopyroxene, orthopyroxene, and plagioclase occur as interstitial grains (Fig. 5*a*). Cr-spinel occurs as inclusions in olivine (Fig. 5*f*). Compared to Pl lherzolite, the pl-ol websterite has a higher proportion of clinopyroxene but a lower proportion of olivine. Olivine gabbronorite is composed of olivine (15-30%), orthopyroxene (5%), clinopyroxene (10-30%), hornblende (10-15%), plagioclase (20-50%), and minor Cr-spinel (<0.5%) (Fig. 5*b*). Gabbronorite is mainly composed of orthopyroxene (10-20%) clinopyroxene (10-15%), plagioclase (45-60%), hornblende (10%), and minor magnetite (Fig. 5*c*). Hb gabbro (Fig. 5*d*) consists of hornblende (25-40%), plagioclase (45-55%), clinopyroxene (5-15%), and minor magnetite (1%). Sulfides of the Dulaan intrusion, which are dominated by pyrrhotite and pentlandite (Fig. 5*f*), occur as small inclusions in olivine (Fig. 5*e*) and hornblende (Fig. 5*f*).

The Nomgon intrusion comprises troctolite, olivine gabbro and gabbro (Izokh et al., 1990). It has no ultramafic rocks outcropping at the surface, and no intrusive contact among different rock types has been observed. Troctolite consists of 15- 20% olivine, 5-10% clinopyroxene, 70-75% plagioclase, and 1-3% magnetite (Fig. 6*a*). Olivine gabbro is composed of 5-15% olivine, 18-35% clinopyroxene, 5-15% hornblende, 45-80% plagioclase, <5% orthopyroxene and minor magnetite (1-5%) (Fig. 6*b*). Olivine gabbro containing a high proportion of olivine and clinopyroxene (generally olivine + clinopyroxene > 50%) is defined as mela-olivine gabbro (Izokh et al., 1990), which is mainly distributed in the central and south rim of the intrusion. Gabbro contains 15-30% clinopyroxene, 5-15% hornblende, 60-70% plagioclase, and 2-5% magnetite (Fig. 6*c*). Rocks with visible sulfides are distributed in many localities within the intrusion (Fig. 3); the largest one is located to the west of the intrusions, close to the contact zone between the intrusion and the country rock. The sulfide assemblage is dominated by chalcopyrite (Fig. 6*d*), whereas pyrrhotite and pentlandite are rare.

Based on the mineral proportions estimated from thin sections, the rock types described above are consistent with the terminology of the International Union of Geological Sciences (IUGS) (Le Maitre et al., 2005) (Fig. 7).

ANALYTICAL METHOD

All samples used in this study were collected from the outcrops and the sample locations are shown in Fig. 2 and 3. The mineral proportion of the samples were estimated at thin-section scale using Zeiss microscope. The concentrations of major elements in olivine, spinel, clinopyroxene were conducted at the Institute of Geology and Geophysics, Chinese Academy of Sciences, Beijing. They were determined by wavelength–dispersive microprobe analysis using a JEOL JXA8100 electron probe. The operating conditions were 15 kV accelerating voltage, 12 nA beam current, 5 μm beam size and 30 s peak counting time. Ni and Ca in olivine were analyzed using a beam current of 40 nA and a peak counting time of 100s. The detection limit for Ni and Ca under such condition is ~150 ppm.

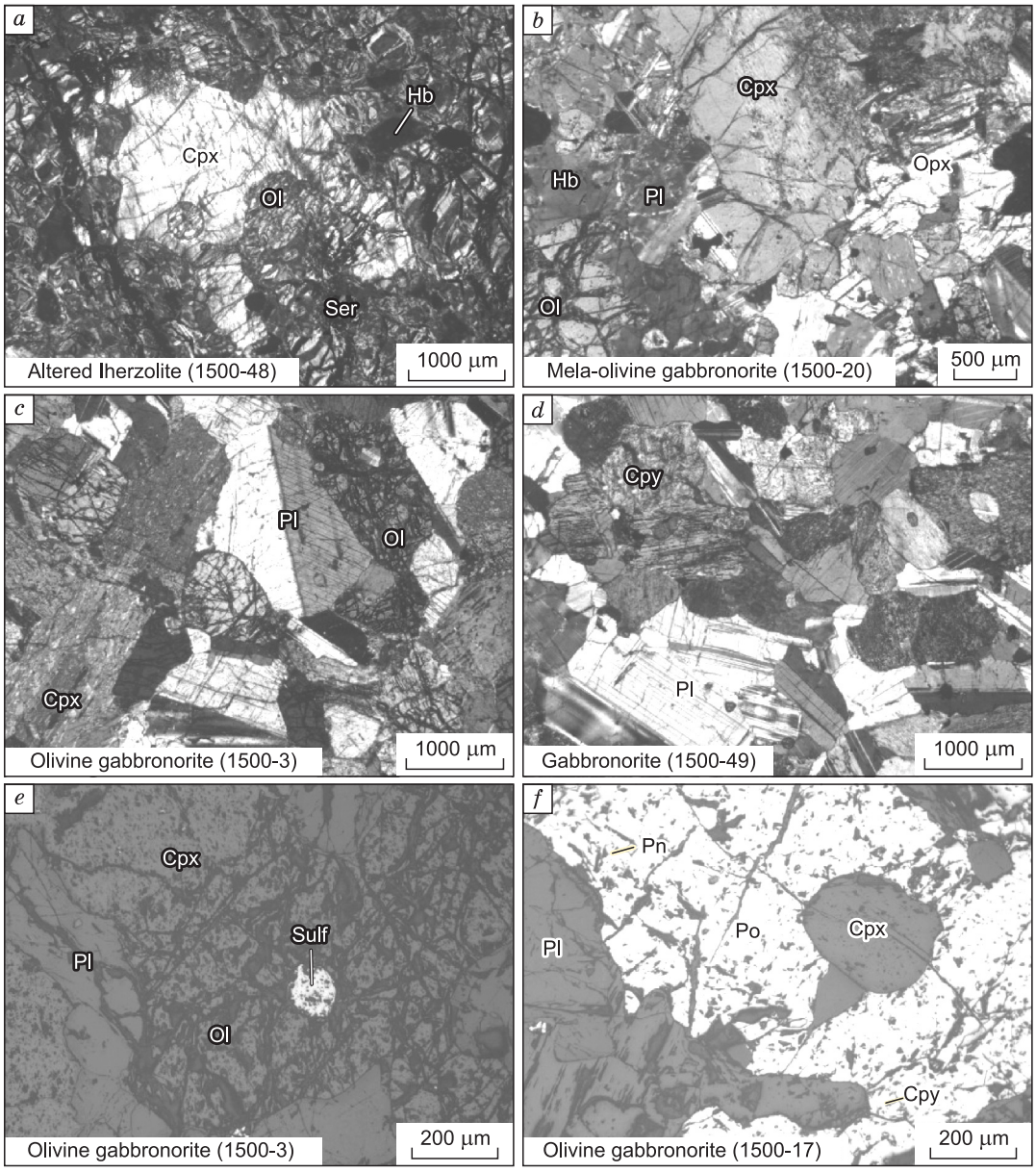

Fig. 4. Photography of rocks from the Oortsog intrusion. (*a*). Altered lherzolite, (*b*). Meta-olivine gabbronorite, (*c*). Olivine gabbronorite, (*d*). Gabbronorite, (*e-f*). Sulfide in olivine gabbronorite.

Abbreviations: Cpx–clinopyroxene, Cpy–chalcopyrite, Hb–hornblende, Ol–olivine, Opx–orthopyroxene, Pl-plagioclase, Po–pyrrhotite, Ser-serpentine, Sul-sulfide.

The abundances of Cu, Ni, and Zr in whole rocks were determined using an ELEMENT inductively coupled plasma mass spectrometry (ICP–MS) of Finnigan MAT at the IGGCAS. 40 mg powders from each sample were dissolved 1 ml HF mixed with 0.5 ml HNO_3 in a Teflon screw–cap capsules at 170°C for 10 days. The sample solutions were then dried and dissolved again in 2 ml HNO_3 in the capsules. Finally, the solutions were diluted with 1% HNO_3 to 50 ml for trace element analysis. The Chinese national standard GSR3 was used to monitor the accuracy and reproducibility. The standard deviation of the standard was better than 3%. The precision was better than 5%. The concentrations of sulfur in rocks were determined using a LECO carbon–sulfur analyzer with a detection limit of 0.01 wt.% in the ALS Chemex laboratory, Guangzhou, China. Rock samples for PGE analyses (~0.5 kg) were ground to <75 μm in size using an agate mill. The concentrations of PGE in sulfide-bearing samples were determined by the combination of NiS-bead pre-concentration, Te co-precipitation, and ICP-MS analysis in the Guangzhou Institute of Geochemistry, Chinese Academy of Sciences on 20 g sample aliquots.

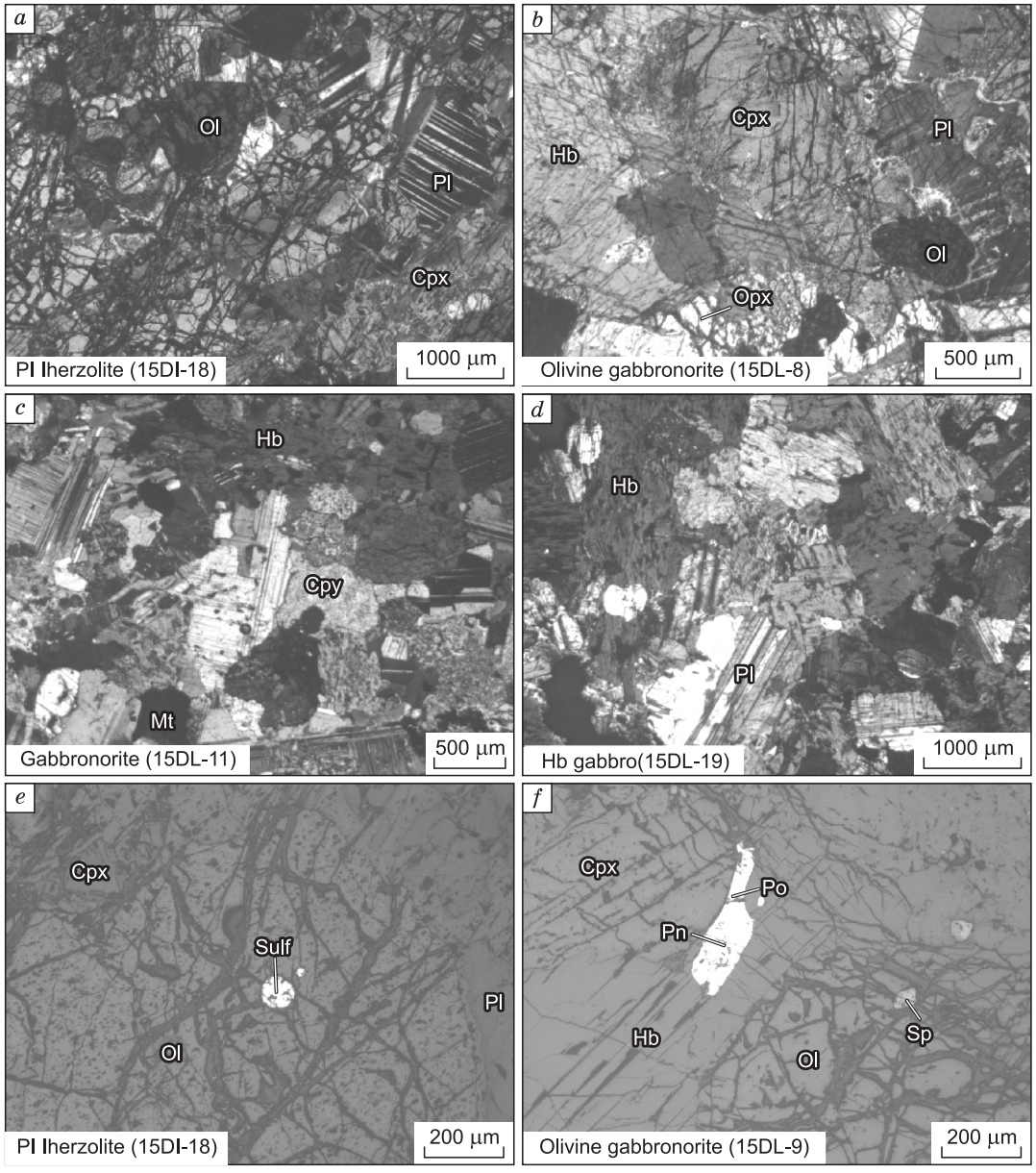

Fig. 5. Photography of rocks from the Dulaan intrusion. (*a*). Pl lherzolite, (*b*). Olivine gabbronorite, (*c*). Gabbronorite, (*d*). Hb gabbro, (*e-f*) Sulfide in Pl lherzolite and olivine gabbronorite. Mt-magnetite, Sp-Cr spinel, others abbreviations are same to Fig. 4.

RESULTS

Olivine composition

The highest Fo value (100*Mg/(Mg+Fe)) and Ni concentration in olivine (82.8 mol.% and 1064 ppm, Table 1) of the Oortsog intrusion are present in lherzolite. The Fo values and Ni contents in olivine of the Oortsog mela-olivine gabbronorite form a relatively narrow range, with Fo values varying from 76.1 to 77.3 and Ni contents varying from 640 ppm to 838 ppm. In contrast, Fo values and Ni contents in olivine from olivine gabbronorite of the Oortsog intrusion vary widely, with Fo values ranging from 70.2 to 79.8 and Ni concentrations ranging from below detection limit to 687 ppm. Fo values and Ni contents in olivine from the Dulaan intrusion vary from 77.6 to 72.9 and from 334 to 1061 ppm, respectively (Table 1). Olivine in mela-olivine gabbronorite of the Dulaan intrusion has relatively higher Fo values and Ni contents than olivine in the Pl lherzolite or the Pl ol websterite. Olivine in troctolite of the Nomgon intrusion records Fo values ranging from 76.3 to 78.3, which are slightly higher than those in olivine gabbro. Nickel contents in olivine of the Nomgon intrusion mainly vary

Table 1. **Composition of olivine from the Oortsog, Dulaan, and Nomgon intrusions in central Mongolia**

No	Sample	Area	Rock type	*n*	SiO_2	MgO	MnO	CaO	FeO	NiO	Total	Fo (mol%)	Ni (ppm)	Ca (ppm)	Mn (ppm)
1	15OO-48	Oortsog	Lherzolite	9	39.0	43.7	0.28	0.02	16.2	0.14	99.4	82.8	1064	176	2171
2	15OO-17	Oortsog	Mela-olivine gabbro	8	38.3	40.0	0.28	0.01	21.2	0.09	99.9	77.1	695	125	2160
3	15OO-18	Oortsog	Mela-olivine gabbro	7	38.3	39.3	0.28	0.02	22.1	0.09	100.1	76.1	712	148	2160
4	15OO-19	Oortsog	Mela-olivine gabbro	13	38.3	40.0	0.28	0.01	21.1	0.08	99.8	77.1	640	113	2147
5	15OO-19-1	Oortsog	Mela-olivine gabbro	3	39.3	40.3	0.26	0.01	21.1	0.11	101.2	77.3	838	111	2006
6	15OO-4	Oortsog	Ol gabbro	8	38.0	38.4	0.33	0.02	22.6	0.09	99.5	75.2	687	174	2531
7	15OO-29	Oortsog	Ol gabbro	8	37.3	35.5	0.36	0.01	26.8	0.01	99.9	70.2	*b.d*	129	2798
8	15OO-1	Oortsog	Ol gabbro	7	38.7	40.3	0.36	0.01	20.7	0.01	100.1	77.6	*b.d*	132	2789
9	15OO-3	Oortsog	Ol gabbro	5	38.4	41.7	0.33	0.02	18.7	0.00	99.2	79.8	*b.d*	162	2546
10	15DL-10	Dulaan	Pl lherzolite	9	38.0	39.4	0.33	0.02	21.6	0.12	99.6	76.5	924	137	2545
11	15DL-10-1	Dulaan	Pl lherzolite	2	38.8	37.7	0.34	0.06	23.4	0.12	100.5	74.2	947	454	2637
12	15DL-18	Dulaan	Pl ol websterite	8	38.0	37.7	0.40	0.01	23.9	0.04	100.1	73.8	334	b.d.	3107
13	15DL-16	Dulaan	Pl ol websterite	7	37.8	37.5	0.36	0.01	23.9	0.08	99.7	73.7	589	113	2809
14	15DL-8	Dulaan	Mela-olivine gabbro	8	38.2	40.2	0.32	0.03	20.6	0.14	99.5	77.6	1061	209	2488
15	15DL-9	Dulaan	Mela-olivine gabbro	8	38.7	39.9	0.31	0.02	21.1	0.13	100.2	77.1	1039	120	2430
16	15DL-14	Dulaan	Ol gabbro	7	38.3	37.1	0.44	0.03	24.6	0.03	100.5	72.9	255	235	3385
17	15DL-17	Dulaan	Ol gabbro	8	37.7	37.4	0.40	0.02	24.3	0.07	100.0	73.3	551	159	3132
18	15NG06	Nomgon	Troctolite	7	38.6	39.8	0.35	0.04	21.3	0.06	100.1	76.9	466	292	2701
19	15NG06-1	Nomgon	Troctolite	4	39.4	39.7	0.34	0.03	21.5	0.05	101.1	76.8	389	241	2670
20	15NG07	Nomgon	Troctolite	8	38.6	40.6	0.32	0.06	20.1	0.06	99.8	78.3	477	402	2493
21	15NG11	Nomgon	Troctolite	8	38.7	39.5	0.36	0.03	21.8	0.05	100.5	76.3	377	244	2757
22	15NG12	Nomgon	Ol gabbro	7	38.5	39.2	0.36	0.03	21.6	0.04	99.8	76.4	314	228	2785
23	15NG14	Nomgon	Ol gabbro	8	38.2	38.3	0.36	0.05	22.3	0.05	99.2	75.4	402	323	2811
24	15NG15	Nomgon	Ol gabbro	8	38.3	38.4	0.35	0.05	22.3	0.14	99.5	75.4	1106	322	2736
25	15NG05	Nomgon	Ol bearing gabbro	4	38.6	40.9	0.37	0.03	19.5	0.01	99.4	78.9	162	179	2862

n: number of analysis, Fo: 100*Mg/(Mg+Fe), b.d: below detection limit

Table 2. **Cr-spinel composition of the Oortsog, Dulaan, and Nomgon intrusions in central Mongolia**

No	Sample	M.A.	Rock type	Mineral	*n*	Cr_2O_3	MgO	MnO	Al_2O_3	FeO	TiO_2	NiO	Total	Fe#	Cr#	$Fe^{3+}/(Fe^{3+}+Cr+Al)$
1	15OO-48	Oortsog	Lherzolite	Sp	7	25.81	5.80	0.40	23.97	40.96	0.94	0.10	98.0	57.7	43.2	7.8
2	15OO-17	Oortsog	Meta ol gabbro	Sp	10	31.08	6.27	0.30	30.24	30.60	0.21	0.02	98.7	54.6	40.9	1.7
3	15OO-19	Oortsog	Meta ol gabbro	Sp	10	29.54	6.72	0.30	31.83	29.61	0.18	0.01	98.2	52.5	38.6	1.6
4	15OO-4	Oortsog	Ol gabbro	Sp	1	12.98	1.6	0.39	5.95	66.0	6.64	0.08	93.6	86.2	59.4	33.6
5	15DL-10	Dulaan	Pl lherzolite	Sp	11	17.62	4.57	0.39	22.06	49.49	3.43	0.11	97.7	68.0	45.8	17.5
6	15DL-8	Dulaan	Meta ol gabbro	Sp	11	24.26	5.07	0.40	26.70	40.90	0.74	0.09	98.1	61.7	38.7	6.7
7	15DL-9	Dulaan	Meta ol gabbro	Sp	14	21.19	4.54	0.40	23.03	47.12	2.09	0.11	98.5	66.7	43.9	12.7

n: number of analysis; Cr#: 100×Cr/(Cr+Al); Fe#: 100×Fe/(Mg+Fe)

from 162 to 477 ppm, but an olivine gabbro (15NG15) records significantly higher concentrations of Ni in olivine (1106 ppm) than other samples. The Ca contents in olivine from these three intrusions are all below 500 ppm.

The Fo values are plotted against Ni and Mn concentrations of the three intrusions in Fig. 8. In this plot, we assume that olivines with Ni contents below the detection limit have a concentration of 150 ppm. Two clusters of olivine compositions have been identified in the Oortsog intrusion (Fig. 8*a*, *b*), in which one has higher Fo values and Mn contents and the other has lower Fo values and Mn contents. The concentrations of Ni in olivine in these two clusters decrease with Fo values, suggesting that the variation between the Ni content and Fo value of each cluster is controlled by olivine fractionation. Similarly, olivines of the Nomgon intrusion plot in two clusters based on their Fo values and Ni content (Fig. 8*a*). In olivine from the Dulaan intrusion, Ni content decreases and Mn content increases with decreasing Fo values (Fig. 8 *a*, *b*), thus indicating a trend of olivine fractionation.

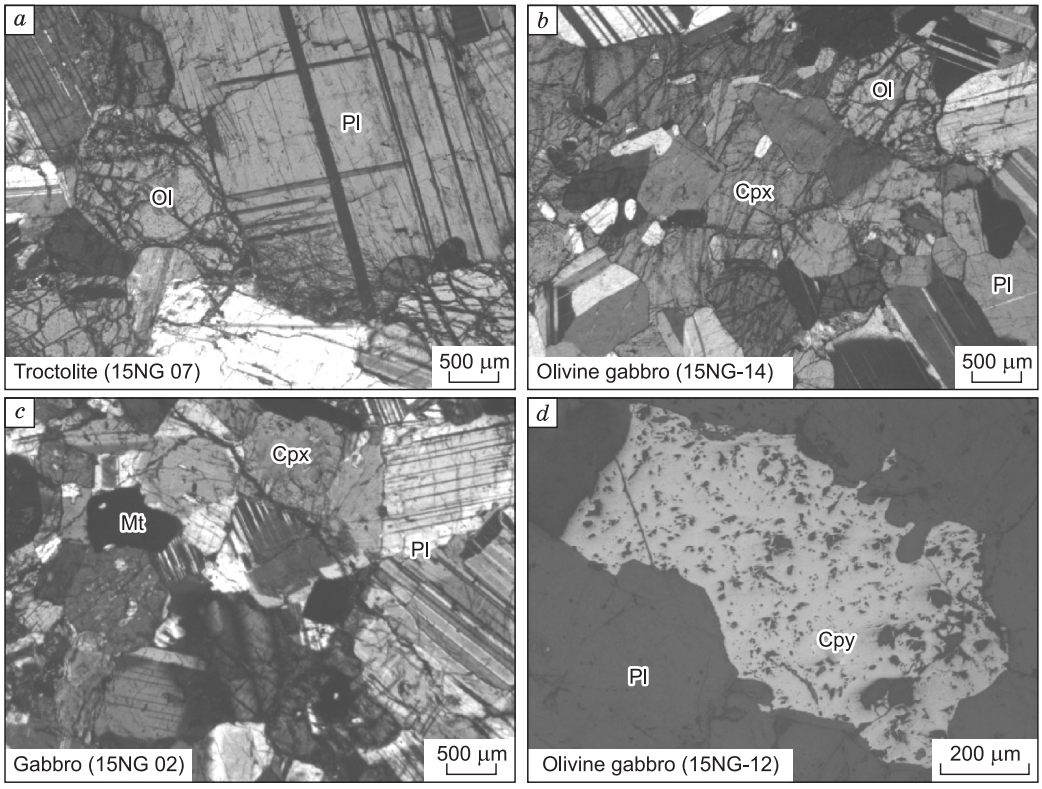

Fig. 6. Photography of rocks from the Nomgon intrusion. (*a*). Troctolite, (*b*). Olivine gabbro, (*c*). Gabbro, (*d*). Chalcopyrite in olivine gabbro. Abbreviations are same to Fig. 4 and Fig. 5.

Cr-spinel composition

The compositions of single Cr-spinel crystals in the Oortsog and Dulaan intrusions vary widely (Table 2). Cr# values (100*Cr/(Cr+Al)) of Cr-spinel from the Oortsog intrusion vary from 30 to 59, whereas those from the Dulaan intrusion vary from 21 to 71. Fe# values (100*Fe^{2+}/(Fe^{2+}+Mg)) of Cr-spinel from the Oortsog intrusion range between 43 and 93, whereas these from the Dulaan intrusion range between 42 and 86. TiO_2 contents in Cr-spinel from the Oortsog intrusion vary from 0.04 to 6.64, whereas those from the Dulaan intrusion vary from 0.04 to 8.02. Fe^{3+}/(Fe^{3+}+Cr+Al) values of Cr-spinel of the Oortsog and Nomgon intrusions range from 1.6 to 41. The Cr-spinel from the Oortsog and Dulaan intrusions follow the Cr-Al trend (Barnes and Roeder,

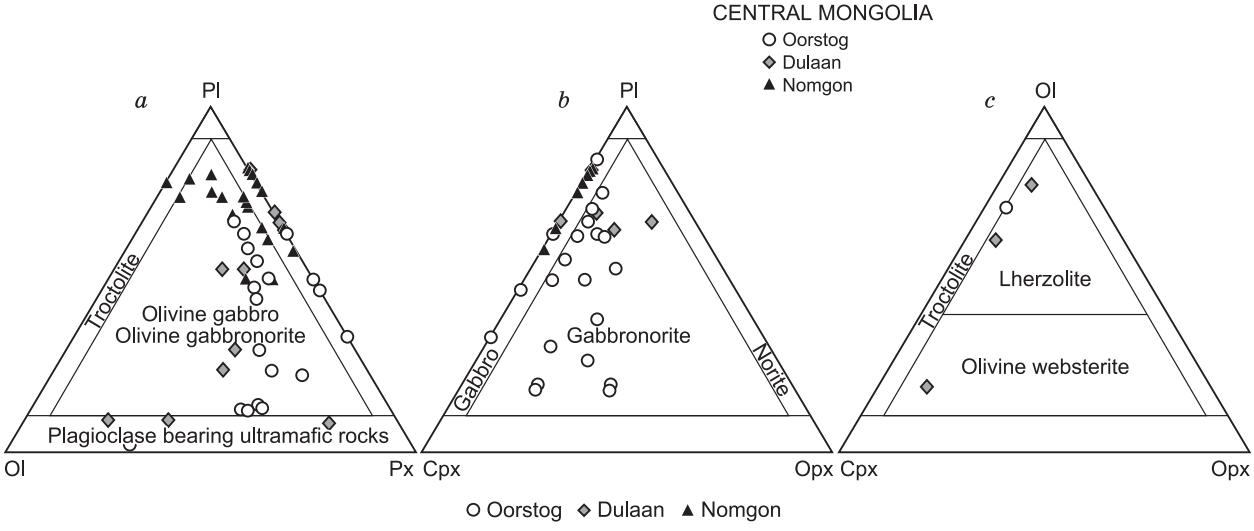

Fig. 7. Rock classification of rocks from the Oortsog, Dulaan and Nomgon intrusions in term of the system of IUGS (Le Maitre et al., 2005).

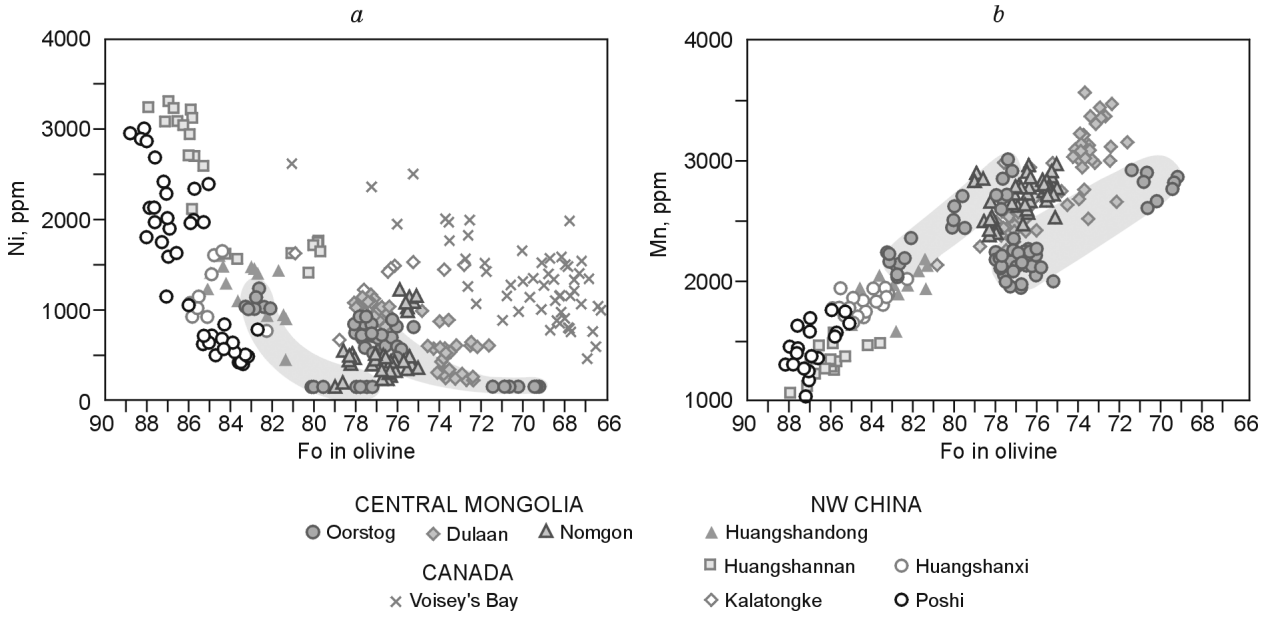

Fig. 8. Compositional variation of olivine from the Oortsog, Dulaan and Nomgon intrusions and comparison with those from magmatic Ni-Cu deposits in NW China and Voisey's Bay deposit in Canada. (*a*) Fo value versus Ni content, (*b*) Fo value versus Mn content, (*c*) Fo value versus Ca content in olivine.

Data source: Oortsog, Dulaan and Nomgon intrusions (this study), Huangshandong (Mao et al., 2015), Huangshannan (Mao et al., 2016), Huangshanxi (Zhang et al., 2011; Mao et al., 2014a); Poshi (Su et al., 2011), Kalatongke (Li et al., 2012), Voisey's Bay (Li et al., 1999), olivine phenocrysts from within plate basalt (Sobolev et al., 2007), olivine from subduction-related magma (Li et al., 2012).

2001), and plot within the region of worldwide tholeiitic basalts (Fig. 9 a-c), with some Cr-spinel plot in the field of island arc basalts (Fig. 9c).

Clinopyroxene composition

In terms of their calculated En, Fs and Wo values (Table 3), the clinopyroxenes of the three intrusions can be classified as diopside and augite. The Mg# values (100*Mg/(Mg+Fe)) of clinopyroxene in lherzolite from the Oortsog intrusion vary from 86 to 89, which are higher than these recorded in the mela-olivine gabbronorite (84 to 86), olivine gabbronorite (79 to 83) and gabbronorite (76 to 86) of the Oortsog intrusion. The variation of Mg# values in clinopyroxene of the Oortsog intrusion is consistent with the variation of Fo values in olivine (Table 1). The Mg# values of clinopyroxene in rocks from the Dulaan intrusion vary from 81 to 87, which is slightly lower than the range recorded in lherzolite from the Oortsog intrusion. The Mg# values in clinopyroxene from rocks in the Nomgon intrusion are lower than those of the Dulaan and Oortsog intrusions. Specifically, troctolite of the Nomgon intrusion has Mg# values ranging from 73 to 81, whereas olivine gabbro and gabbro have slightly higher Mg# values, ranging from 77 to 84 and from 76 to 82, respectively.

On the Al^{IV}–Ti discrimination diagram of clinopyroxene-based magma affinity, clinopyroxene from rocks of the Oortsog and Dulaan intrusions plot along the boundary between tholeiitic magma and calc-alkaline magma, with most of the data points plotting in the field of tholeiitic magma (Fig. 10). In contrast, most of the Nomgon samples plot within the calc-alkaline magma region (Fig. 10).

Whole rock S, Cu, Ni, PGEs and Zr abundances

The whole rock concentrations of S, Cu, Ni, PGE, and Zr are listed in Table 4. Sulfur contents of samples from the Oortsog intrusion vary from 0.09 to 0.58 wt.%, with those from the Dulaan intrusion varying from 0.01 to 0.03 wt.% and those from the Nomgon intrusion varying from 0.09 to 0.58 wt.%. In the Oortsog intrusion, whole rock Zr concentrations range from 3.78 to 39.4 ppm, and the mela-olivine gabbro tends to have higher Zr concentrations than the olivine gabbro (Table 4). In contrast, rocks from the Dulaan and Nomgon intrusions contain lower Zr concentrations than those from the Oortsog intrusion. Rocks from the Nomgon intrusion are substantially enriched in Cu, which ranges from 2197 to 5744 ppm; their S contents vary from 0.22 to 0.58 wt.%. A positive correlation between Ni and S exists in the Oortsog and Nomgon intrusions (Fig. 11*a*), whereas a positive correlation between Cu and S exists in all rocks from the three intrusions (Fig. 11b). Osmium, Ir, and Rh concen-

Table 3. **Clinopyroxene composition of the Oortsog, Dulaan, and Nomgon intrusions in central Mongolia**

No	Sample	Mine area	Rock type	*n*	SiO_2	Cr_2O_3	Na_2O	MgO	MnO	CaO	Al_2O_3	FeO	TiO_2	Total	Mg#	En	Fs	Wo
1	15OO-48	Oortsog	Lherzolite	6	52.0	0.70	0.23	15.8	0.12	22.9	3.32	4.05	0.34	99.5	87.4	45.8	6.6	47.7
2	15OO-17	Oortsog	Meta oll gabbro	8	53.6	0.33	0.35	15.8	0.16	22.7	2.01	4.84	0.18	100.1	85.4	45.4	7.8	46.9
3	15OO-19	Oortsog	Meta oll gabbro	7	53.6	0.33	0.30	16.0	0.16	22.8	1.69	5.01	0.16	100.0	85.0	45.4	8.0	46.6
4	15OO-29	Oortsog	Ol gabbro	6	53.1	0.21	0.23	15.5	0.19	22.7	1.88	5.97	0.31	100.1	82.2	44.0	9.5	46.5
5	15OO-4	Oortsog	Ol gabbro	7	52.5	0.35	0.22	16.2	0.19	20.8	2.54	6.84	0.51	100.2	80.9	46.2	11.0	42.8
6	15OO-52	Oortsog	Gabbro	7	52.9	0.07	0.15	15.7	0.13	23.0	2.39	5.60	0.40	100.4	83.3	44.4	8.9	46.7
7	15DL-10	Dulaan	Pl lherzolite	8	51.4	0.43	0.19	15.5	0.18	22.0	3.81	5.74	0.72	100.0	82.8	44.9	9.3	45.8
8	15DL-18	Dulaan	Pl ol websterite	7	52.9	0.08	0.09	15.6	0.17	24.0	2.18	4.94	0.43	100.4	84.9	43.7	7.8	48.5
9	15DL-8	Dulaan	Meta oll gabbro	9	51.5	0.72	0.14	15.5	0.15	22.4	3.80	5.10	0.43	99.8	84.5	45.1	8.3	46.6
10	15DL-9	Dulaan	Meta oll gabbro	9	51.9	0.68	0.16	15.4	0.15	23.0	3.89	4.54	0.48	100.2	85.8	44.7	7.4	47.9
11	15NG06	Nomgon	Troctolite	9	51.8	0.29	0.30	15.3	0.18	21.5	3.20	7.03	0.64	100.2	79.6	44.2	11.4	44.4
12	15NG07	Nomgon	Troctolite	2	51.9	0.02	0.36	12.9	0.16	23.7	1.73	8.44	0.49	99.7	73.1	37.2	13.7	49.2
13	15NG12	Nomgon	Ol gabbro	5	52.8	0.05	0.24	15.5	0.18	22.7	1.84	6.23	0.32	99.9	81.7	44.0	9.9	46.1
14	15NG14	Nomgon	Ol gabbro	4	50.9	0.28	0.32	14.7	0.17	21.6	3.46	7.25	0.61	99.3	78.3	42.8	11.9	45.3
15	15NG15	Nomgon	Ol gabbro	6	51.0	0.22	0.32	14.8	0.15	21.6	3.31	7.24	0.58	99.3	78.5	43.0	11.8	45.2
16	15NG05	Nomgon	Ol bearing gabbro	5	51.7	0.00	0.29	15.1	0.18	22.3	2.56	6.6	0.52	99.3	80.2	43.3	10.7	46.1
17	15NG02	Nomgon	Gabbro	11	52.7	0.01	0.26	14.3	0.26	23.1	1.79	7.51	0.37	100.3	77.2	40.7	12.0	47.3
18	15NG03	Nomgon	Gabbro(Fine)	10	52.3	0.01	0.29	14.9	0.21	22.7	2.47	6.55	0.49	100.0	80.2	42.6	10.5	46.9

n: number of analysis; Mg#: 100×Mg/(Mg+Fe); Fe#: 100×Fe/(Mg+Fe); Cr#: 100×Cr/(Cr+Al)

trations in the Dulaan intrusion are significantly higher than those in the Oortsog and Nomgon intrusions at similar S contents (Fig. 11*c-e*), but Rh, Pt and Pt concentrations are similar to those in the other intrusions at similar S contents (Fig. 11 *f-h*).

All of the rocks from the three intrusions have Cu/Zr ratios higher than 1 (Table 1, 4).The Ni/Cu ratios of rocks from these intrusions vary significantly. This is because these rocks contain variable proportions of olivine, which record variable concentrations of Ni in olivine. The variations of Cu/Zr and Ni/Cu ratios in rocks with relatively higher S contents (>0.2 wt.%) are much more restricted because the Ni and Cu in these rocks are mainly controlled by sulfide (Fig. 13*a, b*). The Ni/Cu ratios of samples with S contents higher than 0.2 wt.% in the Oortsog intrusion vary from 1.8 to 3.8, which are consistent with the Ni/Cu ratios of the Ni-Cu deposits in NW China (Fig. 13*b*) (Qin et al., 2012). On the other hand, the Ni/Cu ratios (0.03 to 0.07) of rocks with S con-

Table 4. **The PGE, Ni, Cu, and S concentrations in whole-rock of the three intrusions**

No	Sample	Rock type	S	Ni	Cu	Os	Ir	Ru	Rh	Pt	Pd	Zr	Cu/Zr	Ni/Cu
			wt.%			ppb						ppm		
1	1500-4	Ol gabbro	0.09	0.03	0.002	0.08	0.26	0.08	0.40	5.89	5.83	8.21	2.98	12.3
2	1500-29	Ol gabbro	0.47	0.02	0.01	0.04	0.02	0.03	0.02	0.27	0.37	24.0	3.80	1.78
3	1500-17	Mela-ol gabbro	0.58	0.07	0.02	0.21	0.16	0.21	0.10	2.62	2.18	39.4	5.31	3.55
4	1500-18	Mela-ol gabbro	0.34	0.06	0.01	0.19	0.14	0.17	0.10	2.79	2.10	35.0	4.22	3.76
5	1500-19	Mela-ol gabbro	0.37	0.07	0.02	0.22	0.17	0.21	0.16	2.91	2.63	12.4	15.1	3.57
6	15DL-8	Mela-ol gabbro	0.03	0.06	0.003	0.19	0.13	0.10	0.09	1.22	0.91	8.33	3.99	17.1
7	15DL-9	Mela-ol gabbro	0.02	0.06	0.002	0.16	0.18	0.17	0.10	1.10	0.92	6.79	3.63	24.0
8	15DL-10	Pl lherzolite	0.01	0.05	0.001	0.09	0.08	0.09	0.08	0.98	1.13	5.08	1.86	54.1
10	15NG05	Ol bearing gabbro	0.09	0.01	0.000	0.07	0.01	0.02	0.02	2.68	0.94	0.81	5.87	19.6
11	15NG20	Ol bearing gabbro	0.05	0.01	0.02	0.02	0.04	0.02	0.11	7.17	5.99	11.8	14.7	0.38
12	15NG03	Gabbro (fine)	0.02	0.00	0.06	0.02	0.01	0.01	0.02	2.88	1.32	12.4	51.9	0.07
13	15NG11	Troctolite	0.22	0.01	0.22	0.04	0.02	0.02	0.05	2.65	2.19	1.35	1627	0.04
14	15NG14	Ol gabbro	0.58	0.02	0.57	0.10	0.47	0.04	2.23	59.7	11.3	3.6	1576	0.03
15	15NG15	Ol gabbro	0.38	0.03	0.39	0.14	1.03	0.06	4.54	100.2	282.7	5.5	708	0.07
16	15NGZK	Gabbro (coarse)	1.13	0.10	2.38	0.71	0.80	0.84	1.23	26.3	1.80	n.a.	n.a.	n.a.

n.a.:not analyzed

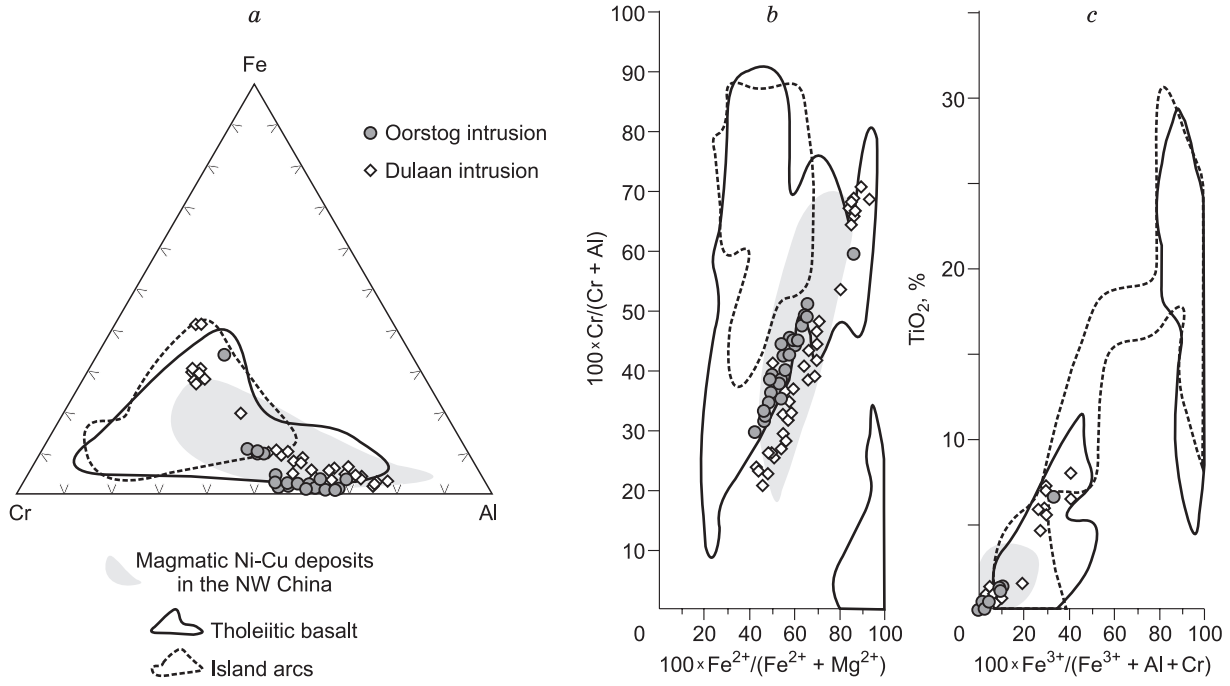

Fig. 9. Compositional variation of Cr-spinel from the Oortsog, Dulaan and Nomgon intrusions and comparison with those from magmatic Ni-Cu deposits in NW China.

Cr-spinel from tholeiitic basalt and arc basalt worldwide (Barnes and Reoder., 2001) are included for comparison. Data source is same to those in Fig. 8.

tents higher than 0.2 wt.% from the Nomgon intrusion are pronouncedly lower than those of the magmatic Ni-Cu deposits (Fig. 13*b*) (Barnes and Lightfoot, 2005).

DISCUSSION

Magma affinities and multiple magma injections of the Oortsog, Dulaan and Nomgon intrusions

Low-Ca concentrations in olivine with high Fo contents are widely used as indicators of mantle origin (Simkin and Smith, 1970). Li et al. (2012) found that olivine in the peridotites of the Annette and Duke Island Complexes in southeastern Alaska also have low Ca contents (<1000 ppm). Subsequently, mafic-ultramafic intrusions in NW China, which were derived from a metasomatized mantle source modified by previous subduction processes (Deng et al., 2015; Mao et al., 2015; Mao et al., 2014a; Xue et al., 2016), have been reported to contain low-Ca olivine. A previous whole rock trace element study of the gabbroids of these intrusions recorded significant depletion in Nb and Ta relative to Th and La (Izokh et al., 1998), which is identical to the trace elemental characteristics of arc magma. Thus, the Oortsog, Dulaan, and Nomgon intrusions could have been formed by parental magmas that are similar to arc magmas or magmas derived from a modified mantle source. Specifically, the parental magmas of the Oortsog and Dulaan intrusions may be tholeiitic, as indicated by the compositions of their Cr-spinel (Fig. 9) and clinopyroxene (Fig. 10). In contrast, the Nomgon intrusion is different than the Oortsog and Dulaan intrusions, and may instead contain clinopyroxene that have crystallized from a magma with calc-alkaline affinity (Fig. 10).

The petrology and grading of mineral proportions within the mafic rocks of the Oortsog,

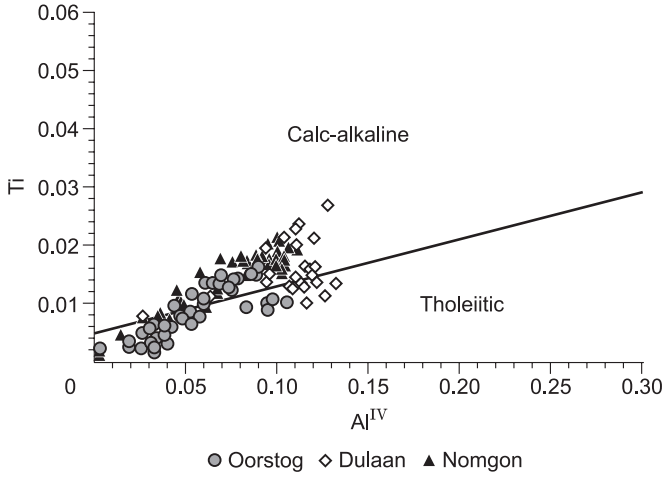

Fig. 10. Al^{IV} versus Ti in Clinopyroxene from the Oortsog, Dulaan, and Nomgon intrusions.

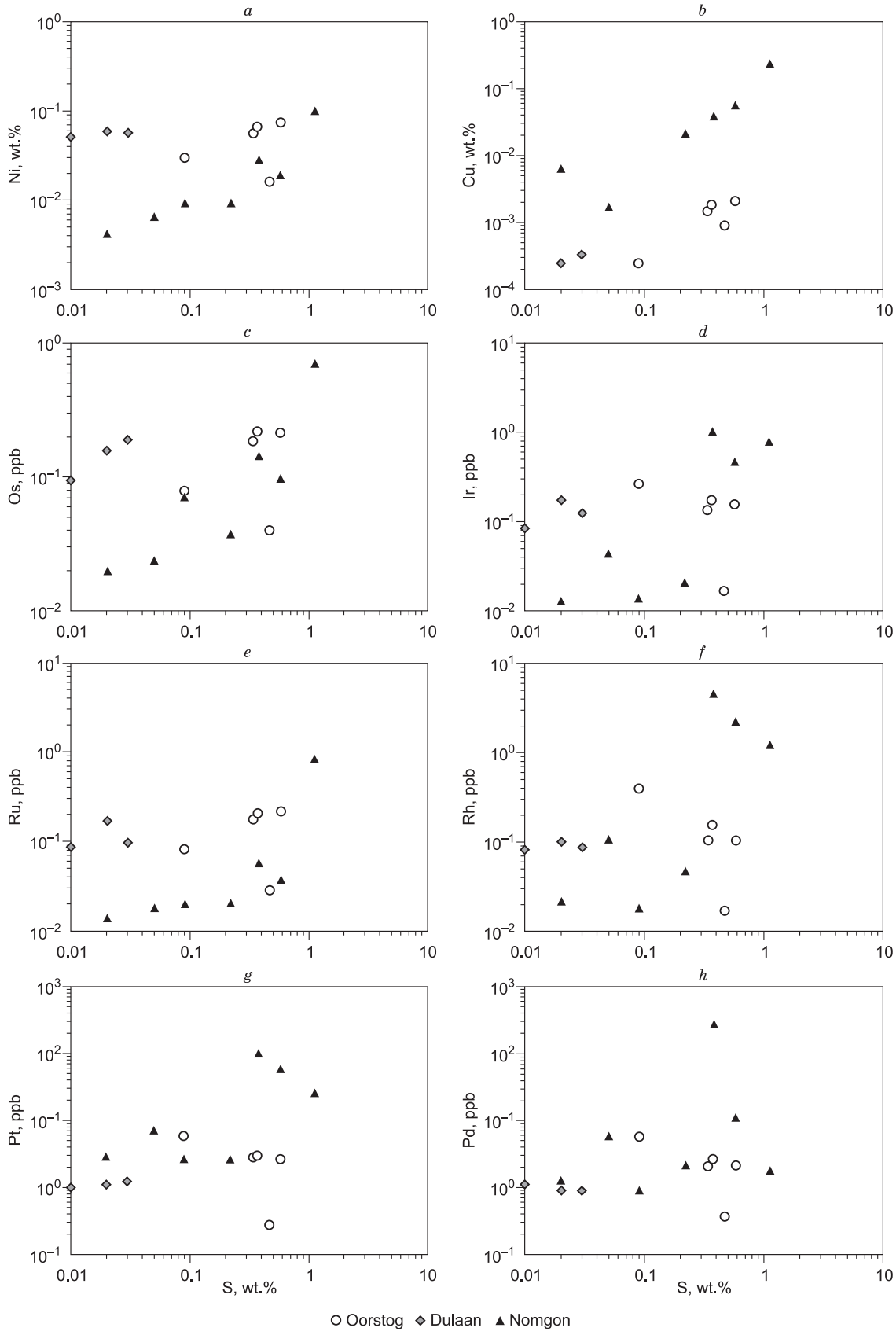

Fig. 11. Sulfur versus Cu/Zr (*a*) and Ni/Cu (*b*) ratios in whole rocks from the Oortsog, Dulaan and Nomgon intrusions. Ni/Cu ratios of Ni-Cu deposit in NW China are from Qin et al. (2012).

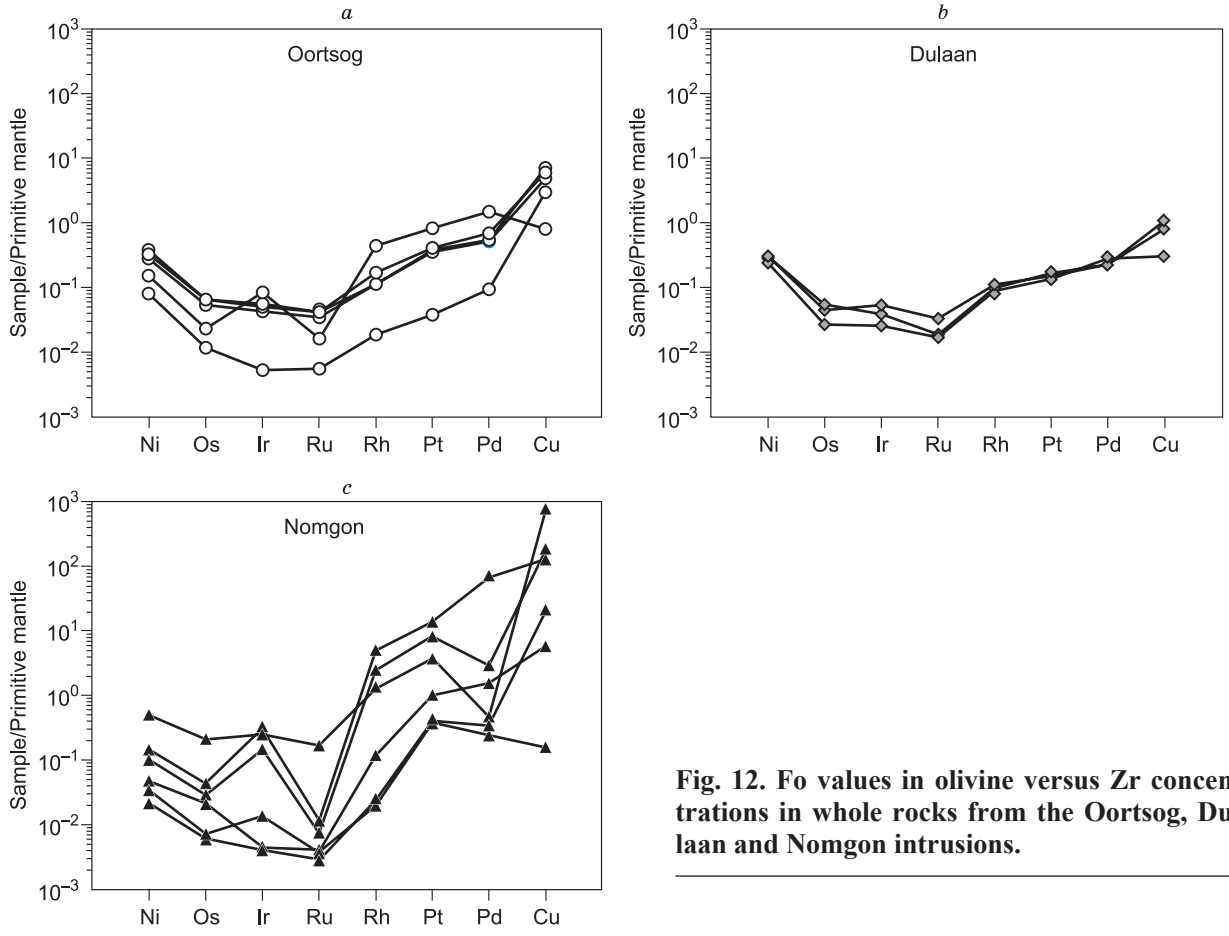

Fig. 12. Fo values in olivine versus Zr concentrations in whole rocks from the Oortsog, Dulaan and Nomgon intrusions.

Dulaan and Nomgon intrusions (Fig. 7) suggest that fractional crystallization has probably played an important role during the emplacement of each intrusion. However, the variations of Fo values with Ni content (Fig. 8a) in the Oortsog and Nomgon intrusions are inconsistent with a fractional crystallization trend. The compositional shift of olivine in the Oortsog intrusion can be explained by either olivine crystallization from multiple magma injections or by interactions with trapped intercumulus liquid. The former process has been identified at numerous mafic-ultramafic intrusions associated with economic Ni-Cu deposits, such as the Huangshandong, Huangshanxi, Limahe and Voisey's Bay Ni-Cu deposits (Li et al., 2001; Mao et al., 2015; Mao et al., 2014a; Tao et al., 2008), while the latter is widely present in layered intrusions and mafic-ultramafic complexes, such as the Voisey's bay and the Jinchuan Ni-Cu deposits and the Stillwater layered intrusion (Barnes, 1986; Li et al., 2000; Li et al., 2004). Furthermore, the Zr concentrations of Nomgon rocks with lower Fo values are significantly higher than those with higher Fo values (Fig. 14, Table 1), indicating that trapped intercumulus liquid may be the cause of the olivine compositional shift. However, the range of Mn in the olivine of the Oortsog intrusion (Fig. 8*b*) cannot be the result of a trapped liquid effect, because Mn is incompatible in olivine (Beattie, 1994), and thus the trapped liquid effect would not significantly decrease the Mn content in olivine. Consequently, multiple magma injections have been proposed to explain the observed olivine compositional variations in the Oortsog intrusion.

Nickel contents and sulfide saturation of the three intrusions

A number of key factors mark the development of a magmatic sulfide deposit, including partial melting of the mantle (producing Ni-bearing magma), ascent into the crust, development of sulfide immiscibility as a result of crustal interaction, concentration, and enrichment of sulfides (Naldrett, 2011). Therefore, the key events governing the development of economic Ni-Cu deposits are the Ni contents of the parental magma and the spatial and temporal development of sulfide saturation in the mantle-derived magma.

To evaluate the Ni contents of the parental magmas of the three intrusions, the olivine compositions of these intrusions are plotted in Fig. 8*a* and compared to those of the Ni-Cu deposits in NW China and the Voisey's Bay. Ni contents in olivine of the three intrusions are slightly lower than those of the magmatic Ni-Cu deposits in NW China (Fig. 8*a*) (Mao et al., 2015; Mao et al., 2014a; Mao et al., 2014b; Xue et al., 2016; Zhang et al., 2011; Zhang et al., 2009), suggesting that their parental magmas are slightly depleted in Ni. Nevertheless,

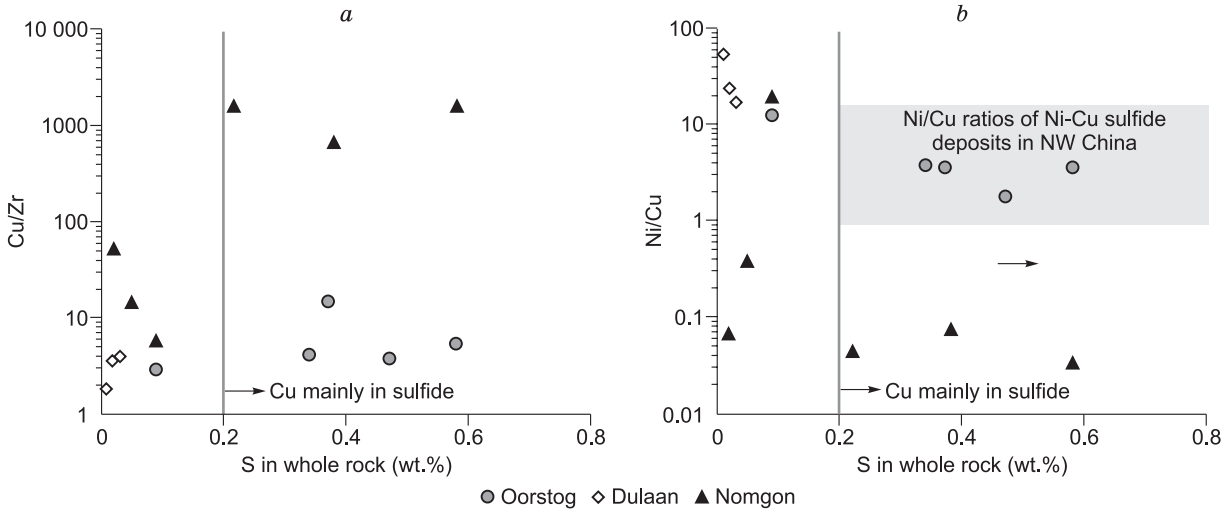

Fig. 13. Sulfur versus Cu/Zr (a) and Ni/Cu (b) ratios in whole rocks from the Oortsog, Dulaan and Nomgon intrusions. Ni/Cu ratios of Ni-Cu deposit in NW China are from Qin et al. (2012).

olivines in lherzolite of the Oortsog intrusion have similar Ni contents and Fo values as those of the Ni-Cu deposits in NW China (Fig. 8*a*) (Mao et al., 2014a). Moreover, the Ni/Cu ratios of rocks from the Oortsog intrusion are identical to those of the Ni-Cu deposits in NW China and worldwide (Fig. 13*b*) (Barnes and Lightfoot, 2005), suggesting that the parental magma of the Oortsog is capable of forming magmatic Ni-Cu deposits. In addition, the parental magma of the Dulaan intrusion may have higher Ni concentrations than that of the Oortsog intrusion, as indicated by its olivine compositions (Fig. 8*a*). In contrast, the extremely low Ni content in olivine of the Nomgon intrusion, combined with the absence of pentlandite in the sulfide phase (Fig. 6), suggests that its parental magma is extremely depleted in Ni but is enriched in Cu.

Furthermore, the analysis of whole rock Cu/Zr ratios can be used to determine whether sulfide segregation occurred in these intrusions (Li and Naldrett, 1999). Because Cu is incompatible in olivine, pyroxene, and plagioclase, the concentration of Cu in whole rock will increase proportionately with that of Zr as fractionation proceeds. However, once sulfide saturation is reached, and sulfide liquids are removed carrying Cu with them, the whole rock Cu/Zr ratio will decrease. If the rock consists cumulus sulfide, the whole rock Cu/Zr will increase. Previous studies of the Noril'sk and Voisey's Bay indicate that the Cu/Zr ratio is a good measure of chalcophile depletion and that samples with Cu/Zr ratios below approximately 1 are well-correlated with sulfide segregation (Li and Naldrett, 1999; Lightfoot and Keays, 2005). The Cu/Zr ratios of rocks of the Oortsog, Dulaan, and Nomgon intrusions are higher than 1 (Fig. 13*a*), suggesting that these rocks contain cumulus sulfide. This indicates that sulfide immiscibility was attained in the magmas of these intrusions. In addition, the presence of rounded sulfide inclusions in olivine gabbro (Fig. 4*e*) of the Oortsog intrusion as well as in plagioclase lherzolite (Fig. 5*e*) of the Dulaan intrusion further indicate that sulfide saturation occurred before or during olivine crystallization.

Origin of the PGE distribution patterns of the three intrusions

The enrichment of Ni and IPGE relative to PPGE in the rocks from the Dulaan intrusion could be the result of IPGE hosted in the olivine cumulate, because IPGE is compatible in olivine (Brenan et al., 2003). This explanation is consistent with petrological observations (Fig. 7*c*). The Os, Ir, and Ru concentrations in rocks from the Oortsog and Nomgon intrusions in-

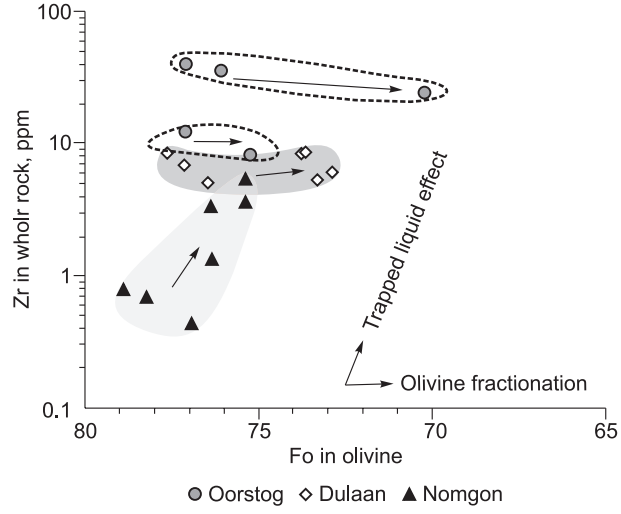

Fig. 14. Fo values in olivine versus Zr concentrations in whole rocks from the Oortsog, Dulaan and Nomgon intrusions.

crease with increasing S concentrations, illustrating that these elements are mainly concentrated in sulfides. In contrast, the Pt and Pd concentrations record a weak correlation with S concentrations (Fig. 11 *g*-*h*), thus indicating that PPGE fractionation or modification by post-magmatic events has occured (Barnes and Lightfoot, 2005). Because the S concentrations in the rocks from the three intrusions are mostly lower than 1 wt.%, the error in the sulfide compositions recalculated from these samples will be remarkably large, as was pointed by Barnes and Lightfoot (2005). Thus, we normalized the whole rocks PGE concentrations to that of the primitive mantle. The primitive mantle-normalized patterns of the rocks from the Oortsog and Dulaan intrusions exhibit slight PPGE enrichment relative to IPGE (Fig. 12*a*-*b*), however, those from the Nomgon intrusion record show significant PPGE enrichment relative to IPGE (Fig. 12*c*). The IPGE depletion in rocks from these intrusions are consistent with the model that IPGEs are compatible in olivine in the mantle and therefore do not reach high concentrations in mantle melts until large degrees of melting have occurred (Mungall et al., 2014), thus implying that these intrusions were derived from a lower degree of partial melting. This is consistent with the estimated degree of partial melting in the magmas related to the Ni-Cu deposits in NW China (Mao et al., 2014a, 2015).

On the other hand, the significantly decoupled PPGE and IPGE in the Nomgon intrusion require an explanation. This trend could be the result of significant olivine fractionation or the removal of IPGE alloy from the parental magma of the Nomgon intrusion at depth. Significant olivine fractionation will produce slightly PPGE-enriched and significantly IPGE-depleted magma, however, the relatively higher Fo values in olivine from the Nomgon intrusion relative to those of the Dulaan intrusion (Fig. 8) suggest that olivine fractionation may not be the key process controlling the PGE patterns of these intrusions. In addition, neither olivine fractionation nor the removal of IPGE alloy from the parental magma could significantly increase the PPGE concentrations of the parental magma. Consequently, the significant PPGE enrichment in the Nomgon intrusion relative to that of the Oortsog and Dulaan intrusions is most likely because these intrusions were formed from two distinctly different magmas, which may have been derived from different degrees of partial melting or by the melting of different mantle sources.

Comparisons between mafic-ultramafic intrusions in central Mongolia and those in NW China

The surface areas of the Oortsog, Dulaan and Nomgon intrusions in central Mongolia are less than 6 km^2, which are slightly larger than those in NW China (<3 km^2) (Qin et al., 2012). However, they all can be defined as small-sized intrusions, based on the definition that small-sized intrusions commonly have surface areas of less than 10 km^2 (Tang, 2002). The Oortsog and Dulaan intrusions are composed of a small proportion of ultramafic rocks and a large proportion of mafic rocks (Fig. 2), whereas the Nomgon intrusion is only composed of mafic rocks (Fig. 3). Generally, the constituent minerals of these intrusions are olivine, orthopyroxene, clinopyroxene, plagioclase, and hornblende. These features of the intrusions in central Mongolia are very similar to those of the mafic-ultramafic intrusions associated with economic Ni-Cu deposits in NW China (Mao et al., 2008; Mao et al., 2014b; Qin et al., 2011; Qin et al., 2012; Sun et al., 2013; Wang et al., 1987; Zhang et al., 2011; Zhou et al., 2004). Furthermore, the presence of hydrous minerals in the intrusions of central Mongolia indicates that their parental magmas are H_2O-bearing, which is also similar to the intrusions in NW China. Water-bearing parental magma is critical to forming magmatic Ni-Cu deposits in NW China, because the presence of H_2O can increase the degree of partial melting of the mantle source and thus increase the Ni concentrations of the parental magmas (Tang et al., 2013).

Furthermore, the intrusions in central Mongolia and NW China are also broadly comparable in terms of their mineral chemistry, such as their Ca content in olivine (Table 1), Al-Ti variations in spinel (Fig. 9) and Ti-Al variations in clinopyroxene (Fig. 10), as well as their PGE patterns (Fig. 12). The similarity between the mafic-ultramafic intrusions in central Mongolia and the Ni-Cu deposits in NW China suggests that these intrusions may have economic Ni-Cu sulfide potential. However, as discussed above, the parental magmas of the intrusions in central Mongolia are relatively evolved, and their Ni contents are slightly lower than those of the parental magmas in NW China. This indicates that a greater volume of magma is required to form magmatic Ni-Cu deposits within the intrusions in central Mongolia.

Exploration implications for economic Ni-Cu-PGE deposits in central Mongolia

The numerous mafic-ultramafic intrusions containing Ni-Cu mineralization in Mongolia (Fig. 1b) (Dejidmaa et al., 2001; Kozakov et al., 2007; Polyakov et al., 2008) represent abundant targets to exploit economic magmatic Ni-Cu deposits. It is important to note that most of these intrusions are dominated by mafic rocks, although some of them comprise ultramafic units (Dejidmaa et al., 2001). Generally, ultramafic rocks that crystallize from tholeiitic picrite (or basalt) are closely associated with magmatic Ni-Cu mineralization in NW China (Mao et al., 2015; Mao et al., 2014a; Xue et al., 2016) as well as worldwide (e.g. Jinchuan, Noril'sk, Kambalda) (Arndt et al., 2005; Chai and Naldrett, 1992; Naldrett, 2004)). These types of magmas commonly

have high temperatures, high Ni contents, low viscosities, and are thus more capable of forming Ni-Cu deposits (Arndt et al., 2005). Once these magmas reach sulfide saturation, the Ni remaining in the magma will quickly be collected by sulfide. Nevertheless, mafic rocks have also been found to host economic Ni-Cu deposits such as the Kalatongke (Song and Li, 2009), Huangshandong (Mao et al., 2015) and Xiangshan (Han et al., 2010; Tang et al., 2013) Ni-Cu deposits in NW China, and the world-class Voisey's Bay deposit in Canada (Li and Naldrett, 1999). To form this type of Ni-Cu deposit, which is produced by evolved magmas, two main factors are required in addition to Ni-bearing magmas that have reached sulfide saturation: (1) a dynamic magmatic system to transport large volumes of sulfide liquid and concentrate them in limited localities and (2) upgrading of metals in the sulfide phase by new magmas that are not depleted in chalcophiles (Li et al., 2001). Accordingly, the mafic intrusions in Mongolia, which formed in dynamic magmatic systems (such as conduit systems), are capable of concentrating sulfide and upgrading the metal contents in sulfide. On the other hand, more attention should be paid to intrusions with high proportions of ultramafic rocks (i.e. higher proportions of olivine, orthopyroxene, and clinopyroxene).

Moreover, the vicinity of major fault zones (i.e. trans-crustal fault) is important to the formation of Ni-Cu deposits, because main faults allow partial melts of the mantle to ascend into the upper crust (Barnes et al., 2016; Naldrett, 1999). This notion is further supported by the observation that Ni-Cu deposits in NW China are distributed adjacent to main faults (Fig. 1b). Overall, as seen in the intrusions in Mongolia and the economic Ni-Cu deposits in NW China, the following characteristics are of critical importance for the further exploration of magmatic Ni-Cu deposits in Mongolia: 1) adjacent to the trans-crustal structure, 2) mantle melts with moderate to high Ni contents, 3) crustal contamination and sulfide addition from crustal rocks, 4) high magma flux to pass through the intrusion and concentrate sulfides in restricted localities, and 5) upgrading of the sulfide by new surges of magma. Thus, further research of the petrology, geometry, geochronology, and geochemistry of these mafic-ultramafic intrusions is of great importance to understand their origin, interactions with crustal rocks, sulfide upgrade processed, and their emplacement process. It is worth noting that rocks from the Nomgon intrusion are enriched in Pt and Pd compared to rocks of similar S contents from the Kalatongke Ni-Cu deposit which contains the highest PGE abundance among the Ni-Cu deposits in NW China. Thus, the PGE potential of mafic intrusions comparable to the Nomgon intrusion are worth further studying.

CONCLUSIONS

Based on the petrology, PGE geochemistry, and chemical compositions of olivine, spinel, and clinopyroxene from the three mafic-ultramafic intrusions in central Mongolia, as well as a comparison of these intrusions to the Ni-Cu mineralized mafic-ultramafic intrusions in NW China, several findings and implications are listed below:

1. The parental magmas of the Oortsog and Dulaan intrusions are slightly depleted in Ni; the parental magma of the Nomgon intrusion is severely depleted in Ni but is significantly enriched in Cu and PPGE.
2. The Oortsog intrusion was formed by multiple magma injections, as is suggested by the chemical compositions of its olivine crystals.
3. The remarkable decoupling between the IPGE and PPGE of the Nomgon intrusion relative to these of the Oortsog and Dulaan intrusions could be the result of different magmas derived from different mantle melts.
4. Mafic-ultramafic intrusions in central Mongolia are comparable to Ni-Cu deposits in NW China, but the intrusions in Mongolia were formed by more evolved parental magmas.
5. Ni-Cu exploration in Mongolia should focus on mafic intrusions formed by high magma flux in a dynamic system and intrusions with high proportions of ultramafic rocks. PGE mineralization may be associated with intrusions similar to the Nomgon intrusion.

Acknowledgement

The analysis of this study is funded by grants from Key Laboratory of Mineral Resources, Institute of Geology and Geophysics, Chinese Academy of Sciences to Dash Batulzii (KLMR2015-02), the Nature Science Foundation of China (grant 41502095, 41030424 and 41472075) and China Postdoctoral Science Foundation (2015M570146). We would like to thank doc. Kh. Gantumur for supporting the field trip in Mongolia, Di Zhang, Wen-Jun Li, and Bing-Yu Gao for their assistance in laboratory work. This manuscript is completed during the visit of Ya–Jing Mao to CSIRO as a post–doctoral fellow funded by the China Scholarship Council. The manuscript has been improved by the useful comments from an anonymous reviewer and A.E. Izokh.

REFERENCES

Arndt, N.T., Lesher, C.M., Czamanske, G.K., 2005. Mantle-derived magmas and magmatic Ni–Cu-(PGE) deposits. Econ. Geol. 100th Anniv. Vol., 5–24.

Badarch, G., Cunningham, D.W., Windley, B.F., 2002. A new terrane subdivision for Mongolia: implications for the Phanerozoic crustal growth of Central Asia. J. Asian Earth Sci. 21, 87–110.

Barnes, S.J., 1986. The effect of trapped liquid crystallization on cumulus mineral compositions in layered intrusions. Contrib. Mineral. Petrol. 93, 524–531.

Barnes, S.-J., Lightfoot, P., 2005. Formation of magmatic nickel-sulfide ore deposits and processses affecting their copper and platinum-group element contents. Econ. Geol. 100th Anniv. Vol., 179–213.

Barnes, S.J., Roeder, P.L., 2001. The range of spinel compositions in terrestrial mafic and ultramafic rocks. J. Petrol. 42, 2279–2302.

Barnes, S.J., Godel, B., Gürer, D., Brenan, J.M., Robertson, J., Paterson, D., 2013. Sulfide-olivine Fe–Ni exchange and the origin of anomalously Ni rich magmatic sulfides. Econ. Geol. 108, 1971–1982.

Barnes, S.J., Cruden, A.R., Arndt, N., Saumur, B.M., 2016. The mineral system approach applied to magmatic Ni–Cu–PGE sulphide deposits. Ore Geol. Rev. 76, 296–316.

Beattie, P., 1994. Trace-element Partitioning with Application to Magmatic Processes Systematics and energetics of trace-element partitioning between olivine and silicate melts: Implications for the nature of mineral/melt partitioning. Chem. Geol. 117, 57–71.

Brenan, J.M., McDonough, W.F., Dalpe, C., 2003. Experimental constraints on the partitioning of rhenium and some platinum-group elements between olivine and silicate melt. Earth Planet. Sci. Lett. 212, 135–150.

Chai, G., Naldrett, A., 1992. The Jinchuan ultramafic intrusion: Cumulate of a high-Mg basaltic magma. J. Petrol. 33, 277–303.

Dejidmaa, G., Bujinkham, B., Evihuu, A., Enkhtuya, B., Ganbaatar, T., Moenkh-Erdene, N., Oyuntuya, N., 2001. Distribution Map of Deposits and Occurrences in Mongolia (at the scale 1:1,000,000). Geological Information Center, Ulaanbaatar.

Deng, Y.-F., Song, X.-Y., Hollings, P., Zhou, T., Yuan, F., Chen, L.-M., Zhang, D., 2015. Role of asthenosphere and lithosphere in the genesis of the Early Permian Huangshan mafic–ultramafic intrusion in the Northern Tianshan, NW China. Lithos 227, 241–254.

Han, C.M., Xiao, W.J., Zhao, G.C., Ao, S.J., Zhang, J.E., Qu, W.J., Du, A.D., 2010. In-situ U-Pb, Hf and Re-Os isotopic analyses of the Xiangshan Ni–Cu-Co deposit in Eastern Tianshan (Xinjiang), Central Asia Orogenic Belt Constraints on the timing and genesis of the mineralization. Lithos 120, 547–562.

Izokh, A.E., Polyakov, G.V., Krivenko, A.P., Bognibov, V.I., Bayarbileg, L., 1990. The Gabbro Formations of Western Mongolia [in Russian]. Nauka, Novosibirsk.

Izokh, A.E., Polyakov, G.V., Gibsher, A.S., Balykin, P.A., Zhuravlev, D.Z., Parkhomenko, V.A., 1998. High-alumina stratified gabbroids of the Central-Asian fold belt: Geochemistry, Sm–Nd isotopic age, and geodynamic conditions of formation. Geologiya i Geofizika (Soviet Geology and Geophysics) 39 (11), 1565–1577 (1578–1585).

Jahn, B.-M., Capdevila, R., Liu, D., Vernon, A., Badarch, G., 2004. Sources of Phanerozoic granitoids in the transect Bayanhongor–Ulaan Baatar, Mongolia: geochemical and Nd isotopic evidence, and implications for Phanerozoic crustal growth. J. Asian Earth Sci. 23, 629–653.

Kelty, T.K., Yin, A., Dash, B., Gehrels, G.E., Ribeiro, A.E., 2008. Detrital-zircon geochronology of Paleozoic sedimentary rocks in the Hangay–Hentey basin, north-central Mongolia: Implications for the tectonic evolution of the Mongol–Okhotsk Ocean in central Asia. Tectonophysics 451, 290–311.

Kozakov, I.K., Sal'nikova, E.B., Wang, T., Didenko, A.N., Plotkina, Y.V., Podkovyrov, V.N., 2007. Early Precambrian crystalline complexes of the Central Asian microcontinent: Age, sources, tectonic position. Stratigr. Geol. Correl. 15, 121–140.

Le Maitre, R.W., Streckeisen, A., Zanettin, B., Le Bas, M., Bonin, B., Bateman, P., 2005. Igneous Rocks: A Classification and Glossary of Terms: Recommendations of the International Union of Geological Sciences Subcommission on the Systematics of Igneous Rocks. Cambridge University Press, Cambridge.

Li, C., Naldrett, A.J., 1999. Geology and petrology of the Voisey's Bay intrusion: reaction of olivine with sulfide and silicate liquids. Lithos 47, 1–31.

Li, C., Lightfoot, P.C., Amelin, Y., Naldrett, A.J., 2000. Contrasting petrological and geochemical relationships in the Voisey's Bay and Mushuau intrusions, Labrador, Canada: Implications for ore genesis. Econ. Geol. 95, 771–799.

Li, C., Naldrett, A.J., Ripley, E.M., 2001. Critical factors for the formation of a nickel-copper deposit in an evolved magma system: lessons from a comparison of the Pants Lake and Voisey's Bay sulfide occurrences in Labrador, Canada. Miner. Deposita 36, 85–92.

Li, C., Xu, Z., de Waal, S.A., Ripley, E.M., Maier, W.D., 2004. Compositional variations of olivine from the Jinchuan Ni–Cu sulfide deposit, western China: implications for ore genesis. Miner. Deposita 39, 159–172.

Li, C., Naldrett, A.J., Ripley, E.M., 2007. Controls on the Fo and Ni contents of olivine in sulfide-bearing mafic/ultramafic intrusions: Principles, modeling, and examples from Voisey's Bay. Earth Sci. Frontiers 14, 177–183.

Li, C., Thakurta, J., Ripley, E., 2012. Low-Ca contents and kink-banded textures are not unique to mantle olivine: evidence from the Duke Island Complex, Alaska. Miner. Petrol. 104, 147–153.

Li, C., Zhang, Z., Li, W., Wang, Y., Sun, T., Ripley, E.M., 2015. Geochronology, petrology and Hf–S isotope geochemistry of the newly-discovered Xiarihamu magmatic Ni–Cu sulfide deposit in the Qinghai–Tibet plateau, western China. Lithos 216–217, 224–240.

Lightfoot, P.C., Keays, R.R., 2005. Siderophile and chalcophile metal variations in flood basalts from the Siberian trap, Noril'sk Region: Implications for the origin of the Ni–Cu–PGE sulfide ores. Econ. Geol. 100, 439–462.

Maier, W.D., Barnes, S.J., Chinyepi, G., Barton Jr, J.M., Eglington, B., Setshedi, I., 2008. The composition of magmatic Ni–Cu–(PGE) sulfide deposits in the Tati and Selebi-Phikwe belts of eastern Botswana. Miner. Deposita 43, 37–60.

Maier, W.D., Smithies, R.H., Spaggiari, C.V., Barnes, S.J., Kirkland, C.L., Yang, S., Lahaye, Y., Kiddie, O., MacRae, C., 2016. Petrogenesis and Ni–Cu sulphide potential of mafic–ultramafic rocks in the Mesoproterozoic Fraser Zone within the Albany-Fraser Orogen, Western Australia. Precambrian Res. 281, 27–46.

Mao, J.W., Pirajno, F., Zhang, Z.H., Chai, F.M., Wu, H., Chen, S.P., Cheng, L.S., Yang, J.M., Zhang, C.Q., 2008. A review of the Cu-Ni sulphide deposits in the Chinese Tianshan and Altay orogens (Xinjiang Autonomous Region, NW China): Principal characteristics and ore-forming processes. J. Asian Earth Sci. 32, 184–203.

Mao, Y.-J., Qin, K.-Z., Li, C., Xue, S.C., Ripley, E.M., 2014a. Petrogenesis and ore genesis of the Permian Huangshanxi sulfide ore-bearing mafic–ultramafic intrusion in the Central Asian Orogenic Belt, western China. Lithos 200, 111–125.

Mao, Y.-J., Qin, K.-Z., Tang, D.M., Xue, S.C., Feng, H.Y., Tian, Y., 2014b. Multiple stages of magma emplacement and mineralization of eastern Tianshan, Xinjiang: Examplified by the Huangshan Ni–Cu deposit. Acta Petrol. Sin. 30, 1575–1594.

Mao, Y.-J., Qin, K.-Z., Li, C., Tang, D.-M., 2015. A modified genetic model for the Huangshandong magmatic sulfide deposit in the Central Asian Orogenic Belt, Xinjiang, western China. Miner. Deposita 50, 65–82.

Mungall, J.E., Brenan, J.M., 2014. Partitioning of platinum-group elements and Au between sulfide liquid and basalt and the origins of mantle-crust fractionation of the chalcophile elements. Geochim. Cosmochim. Acta 125, 265–289.

Naldrett, A.J., 1999. World-class Ni–Cu-PGE deposits: key factors in their genesis. Miner. Deposita 34, 227–240.

Naldrett, A.J., 2004. Magmatic Sulfide Deposits: Geology, Geochemistry and Exploration. Springer.

Naldrett, A.J., 2010a. From the mantle to the bank: The life of a Ni–Cu–(PGE) sulfide deposit. S Afr. J. Geol. 113, 1–32.

Naldrett, A.J., 2010b. Secular variation of magmatic sulfide deposits and their source magmas. Econ. Geol. 105, 669–688.

Naldrett, A.J., 2011. Fundamentals of magmatic sulfide deposits, in: Li, C., Ripley, E. (Eds.), Magmatic Ni–Cu and PGE Deposits: Geology, Geochemistry and Genesis. Society of Economic Geologists, Denver, Colorado, pp. 1–50.

Oyunchimeg, T., Izokh, A.E., Vishnevsky, A.V., Kalugin, V.M., 2009. Isoferroplatinum mineral assemblage from the Burgastain Gol placer (Western Mongolia). Russian Geology and Geophysics (Geologiya i Geofizika) 50 (10), 863–872 (119–1130).

Polyakov, G.V., Izokh, A.E., Borisenko, A.S., 2008. Permian ultramafic-mafic magmatism and accompanying Cu-Ni mineralization in the Gobi-Tien Shan belt as a result of the Tarim plume activity. Russian Geology and Geophysics (Geologiya i Geofizika) 49 (7), 455–467 (605–620).

Qin, K.-Z., Zhang, L.-C., Xiao, W., Xu, X., Yan, Z., Mao, J., 2003. Overview of major Au, Cu, Ni and Fe deposits and metallogenic evolution of the eastern Tianshan Mountains, Northwestern China, in: Mao, J.W., Goldfarb, R.J., Seltmann, R., Wang, D.W., Xiao, W.J., Hart, C. (Eds.), Tectonic Evolution and Metallogeny of the Chinese Altay and Tianshan. International Association on the Genesis of Ore Deposits and CERCAMS, London, pp. 227–249.

Qin, K.-Z., Su, B.-X., Sakyi, P.A., Tang, D.M., Li, X.H., Sun, H., Xiao, Q.H., Liu, P.P., 2011. Sims zircon U–Pb geochronology and Sr-Nd isotopes of Ni–Cu-bearing mafic–ultramafic intrusions in Eastern tianshan and Beishan in correlation with flood basalts in Tarim basin (NW China): Constraints on a Ca. 280 Ma mantle plume. Am. J. Sci. 311, 237–260.

Qin, K.-Z., Tang, D.-M., Su, B.-X., Mao, Y.-J., Xue, S.-C., 2012. The tectonic setting, stytle, basic feature, relative erosion degree, ore-bearing evaluation sign, potential analysis of mineralization of Cu-Ni bearing Permian mafic–ultramafic complexes, Northern Xinjiang. Northwest. Geol. 45, 83–116.

Sengör, A., Natal'in, B., Burtman, V., 1993. Evolution of the Altaid tectonic collage and Palaeozoic crustal growth in Eurasia. Nature 364, 299–307.

Sengör, A.M.C., Natalin, B.A., 1996. Paleotectonics of Asia: fragments of a synthesis, in: Yin, A., Harrison, M. (Eds.), The Tectonic Evolution of Asia. Cambridge University Press, Cambridge, pp. 486–641.

Shelepaev, R., Vishnevsky, A., Izokh, A., Egorova, V., Shelepov, Y., 2015. Permian maifc complexes of the Khangai Region (Western Mongolia), in: First China-Russia International Meeting on the Central Asian Orogenic Belt and IGCP 592 Workshop. Institute of Geology, Chinese Academy of Geological Sciences, Beijing, pp. 78–79.

Simkin, T., Smith, J.V., 1970. Minor-element distribution in olivine. J. Geol. 78, 304–325.

Sobolev, A.V., Hofmann, A.W., Kuzmin, D.V., Yaxley, G.M., Arndt, N.T., Chung, S.L., Danyushevsky, L.V., Elliott, T., Frey, F.A., Garcia, M.O., Gurenko, A.A., Kamenetsky, V.S., Kerr, A.C., Krivolutskaya, N.A., Matvienkov, V.V., Nikogosian, I.K., Rocholl, A., Sigurdsson, I.A., Sushchevskaya, N.M., Teklay, M., 2007. The amount of recycled crust in sources of mantle-derived melts. Science 316, 412–417.

Song, X.Y., Li, X.R., 2009. Geochemistry of the Kalatongke Ni–Cu-(PGE) sulfide deposit, NW China: implications for the formation of magmatic sulfide mineralization in a postcollisional environment. Miner. Deposita 44, 303–327.

Su, B.-X., Qin, K.-Z., Sakyi, P.A., Li, X.-H., Yang, Y.-H., Sun, H., Tang, D.-M., Liu, P.-P., Xiao, Q.-H., Malaviarachchi, S.P.K., 2011. U–Pb ages and Hf–O isotopes of zircons from Late Paleozoic mafic–ultramafic units in the southern Central Asian Orogenic Belt: Tectonic implications and evidence for an Early-Permian mantle plume. Gondwana Res. 20, 516–531.

Sun, T., Qian, Z.Z., Deng, Y.F., Li, C.S., Song, X.Y., Tang, Q.Y., 2013. PGE and isotope (Hf–Sr–Nd–Pb) constraints on the origin of the Huangshandong magmatic Ni–Cu sulfide deposit in the Central Asian Orogenic Belt, northwestern China. Econ. Geol. 108, 1849–1864.

Tang, D.M., Qin, K.Z., Li, C., Qi, L., Su, B.X., Qu, W.J., 2011. Zircon dating, Hf–Sr–Nd–Os isotopes and PGE geochemistry of the Tianyu sulfide-bearing mafic–ultramafic intrusion in the Central Asian Orogenic Belt, NW China. Lithos 126, 84–98.

Tang, D., Qin, K., Su, B., Sakyi, P.A., Liu, Y., Mao, Q., Santosh, M., Ma, Y., 2013. Magma source and tectonics of the Xiangshanzhong mafic–ultramafic intrusion in the Central Asian Orogenic Belt, NW China, traced from geochemical and isotopic signatures. Lithos 170–171, 144–163.

Tang, Z., 2002. Magmatic ore deposits in small rockbody in China. Eng. Sci. 4, 9–12.

Tao, Y., Li, C., Song, X.-Y., Ripley, E., 2008. Mineralogical, petrological, and geochemical studies of the Limahe mafic–ultramatic intrusion and associated Ni–Cu sulfide ores, SW China. Miner. Deposita 43, 849–872.

Wang, R.M., Liu, D.Q., Yin, D.T., 1987. The conditions of controlling metallogny of Cu-Ni sulfide ore deposits and the orientation of finding ore Hami, Xinjiang, China. J. Mineral. Petrol. 7, 1–152.

Wei, B., Wang, C.Y., Li, C., Sun, Y., 2013. Origin of PGE-depleted Ni–Cu sulfide mineralization in the Triassic Hongqiling No. 7 orthopyroxenite intrusion, Central Asian Orogenic Belt, northeastern China. Econ. Geol. 108, 1813–1831.

Wei, B., Wang, C.Y., Arndt, N.T., Prichard, H.M., Fisher, P.C., 2015. Textural relationship of sulfide ores, PGE, and Sr–Nd–Os isotope compositions of the Triassic Piaohechuan Ni–Cu Sulfide Deposit in NE China. Econ. Geol. 110, 2041–2062.

Windley, B.F., Alexeiev, D., Xiao, W., Kröner, A., Badarch, G., 2007. Tectonic models for accretion of the Central Asian Orogenic Belt. J. Geol. Soc. 164, 31–47.

Xia, M.-Z., Jiang, C.-Y., Li, C., Xia, Z.-D., 2013. Characteristics of a newly discovered Ni–Cu sulfide deposit hosted in the Poyi ultramafic intrusion, Tarim Craton, NW China. Econ. Geol. 108, 1865–1878.

Xiao, W.J., Zhang, L.C., Qin, K.Z., Sun, S., Li, J.L., 2004. Paleozoic accretionary and collisional tectonics of the Eastern Tianshan (China): Implications for the continental growth of Central Asia. Am. J. Sci. 304, 370–395.

Xie, W., Song, X.-Y., Deng, Y.-F., Wang, Y.-S., Ba, D.-H., Zheng, W.-Q., Li, X.-B., 2012. Geochemistry and petrogenetic implications of a Late Devonian mafic–ultramafic intrusion at the southern margin of the Central Asian Orogenic Belt. Lithos 144–145, 209–230.

Xue, S., Qin, K., Li, C., Tang, D., Mao, Y., Qi, L., Ripley, E.M., 2016. Geochronological, petrological and geochemical constraints on Ni–Cu sulfide mineralization in the Poyi ultramafic-troctolitic intrusion in the NE rim of Tarim Craton, Western China. Econ. Geol. 111 (6), 1465–1484.

Yarmolyuk, V., Kovalenko, V., 1991. Rift Magmatism of Active Continental Margins and its Ore Potential [in Russian]. Nauka, Moscow.

Zhang, M., Li, C., Fu, P., Hu, P., Ripley, E., 2011. The Permian Huangshanxi Cu–Ni deposit in western China: intrusive–extrusive association, ore genesis, and exploration implications. Miner. Deposita 46, 153–170.

Zhang, Z.C., Mao, J.W., Chai, F.M., Yan, S.H., Chen, B.L., Pirajno, F., 2009. Geochemistry of the Permian Kalatongke mafic intrusions, northern Xinjiang, Northwest China: Implications for the genesis of magmatic Ni–Cu sulfide deposits. Econ. Geol. 104, 185–203.

Zhou, M.F., Lesher, C.M., Yang, Z.X., Li, J.W., Sun, M., 2004. Geochemistry and petrogenesis of 270 Ma Ni–Cu-(PGE) sulfide-bearing mafic intrusions in the Huangshan district, Eastern Xinjiang, Northwest China: implications for the tectonic evolution of the Central Asian orogenic belt. Chem. Geol. 209, 233–257.

Рекомендована к печати 8 февраля 2017 г.
А.Э. Изохом

Поступила в редакцию
19 июля 2016 г.